Department of the Navy
BUREAU OF YARDS AND DOCKS
Contract NOy-12561

BREAKING WAVE FORCES ON PLANE BARRIERS

John H. Carr

Hydrodynamics Laboratory
Hydraulic Structures Division
CALIFORNIA INSTITUTE OF TECHNOLOGY
Pasadena, California

Report No. E-11.3
November, 1954

Project Supervisor:
John H. Carr

Department of the Navy

Bureau of Yards and Docks

Contract NOy-12561

BREAKING WAVE FORCES ON PLANE BARRIERS

John H. Carr

Hydrodynamics Laboratory
Hydraulic Structures Division
California Institute of Technology
Pasadena, California

Report No. E-11.3
November, 1954

John H. Carr
Project Supervisor

CONTENTS

SYMBOLS

a	acceleration
α	coefficient with dimensions $1/T$ in exponential decrement formula
c.p.	distance along barrier from toe of barrier to center of pressure of wave forces
C	wave velocity
d	water depth, measured from still water level
d_1	depth of water at toe of barrier
d_b	depth of water where wave breaks
D	undetermined thickness of air cushion for breaking wave (Bagnold's formula)
D_1	depth at foot of foreshore slope in Minikin's formula
e	base of natural logarithms
f	frequency of oscillating system, cycles per sec
F	force
F_1	absolute value of force corresponding to first positive peak of force-time record
F_2	absolute value of force corresponding to first negative peak of force-time record
F_i	value of force in impulse loading
F_o	value of force in step function loading
g	acceleration of gravity
h	height of area over which pressure acts
H	wave height
H_b	height of breaking wave
H_o	wave height in deep water
I	shock impulse recorded with balance apparatus
k	spring constant in force per unit displacement
L	wavelength

L_o wavelength in deep water

m mass

n deflection of recording pen when a load, N, is applied to balance system

N static load applied during calibration of balance system

p pressure

Q the volume of water per unit width of wave crest which is advancing with wave velocity

ρ mass density of water

S width of wave crest between adjacent orthogonals

S_b width of wave crest between adjacent orthogonals where wave breaks

S_o width of wave crest between adjacent orthogonals in deep water

SWL still water level

t time

t_o interval of time during which F_i is maintained

T natural period of oscillator or of wave

U momentum per wave per unit width of crest

u velocity of breaking wave at impact

U_b momentum per wave per unit width of crest when wave starts to break

v velocity

v_o velocity acquired by oscillator after force has been applied for a short time

x displacement of oscillator

x_1 maximum value of displacement of oscillator

x_2 minimum value of displacement of oscillator

x_n deflection of oscillator produced by a static load of N force units

I. INTRODUCTION

For the past twenty-four months this Laboratory has been engaged in a study of wave action on barriers. The first half of this investigation was limited to cases of wave reflection from various structures. The experimental program for this first phase of the investigation included both the development of instrumentation and experimental techniques and the measurement of wave forces and pressures acting on plane barriers inclined at various angles and on a family of curved and stepped-face barriers selected by the Bureau of Yards and Docks. The results of that program (Refs. 1 and 2) include:

(1) The development and experimental verification of relatively simple analytical expressions for the force and pressure distributions exerted on vertical plane barriers by reflecting waves. These expressions include a second-order double wave frequency term which becomes of increasing importance for small values of L/d (wavelength to water depth ratio), and which has not heretofore been considered in connection with wave forces on barriers.

(2) The demonstration of a simple relationship between the forces acting on a vertical plane barrier and those acting on plane barriers inclined at angles up to 30° from the vertical, and on certain curved and stepped-face barrier profiles.

The extension of the program to include the study of breaking waves was a logical consequence of the earlier work, both because of the engineering importance of the breaking wave problem and because the apparatus and experience developed in the first phase promised to be directly applicable to such a study. Previous knowledge of the breaking wave problem was limited almost solely to analysis and measurements of the impulsive or shock pressures developed by breaking waves. Since these short-duration, high-intensity pressures appear in some respects to be unrealistic as the basis for design, this investigation approached the problem by determining the force-time history during the entire wave cycle to permit the evaluation of other aspects of the force function than the singular one of initial impulse.

The study was necessarily restricted to a few values of geometric and wave parameters, but the results, as expressed in dimensionless parameters, promise to provide useful data for a wide range of design problems.

These results include:

(1) Determination of wave steepness and water depth parameters which result in wave breaking for various plane barrier and foreshore geometries.

(2) The correlation of measured breaking wave impulse with computed wave momentum derived from solitary wave theory.

(3) Experimental determinations of the relationship between wave parameters and the magnitude and location of a maximum effective force believed valid for design purposes, expressed in terms of the computed wave momentum.

II. SUMMARY OF PREVIOUS INVESTIGATIONS

A. Field Investigations

D. D. Gaillard investigated wave pressures with a spring dynamometer at locations in Florida and on the Great Lakes in the years 1890-1902 and in 1915.[3] Other investigations[4,5,6] have used Gaillard's results in connection with the development of theoretical and semi-empirical formulas relating wave height and maximum dynamic pressure. All of these developments have been in the form of expressions for the dynamic pressure developed by a stream of water impinging on a stationary surface. Such calculations have been in notably good agreement with Gaillard's measurements. However, it must be pointed out that pressures calculated on the basis outlined above are valid only for a steady flow process, and this approach does not consider the transient pressures developed before steady flow is established. Similarly, Gaillard's apparatus was undoubtedly incapable of response to impulsive or suddenly applied pressures, hence it is not surprising that theory and experiment agree in these cases, but the results must be regarded only as indicative of some average pressure of long-time duration, and not as the maximum pressure of structural significance.

Rouville and Petry[7] investigated wave pressures at Dieppe in 1933-35, using apparatus capable of relatively high frequency response. Pressures other than the nearly hydrostatic values typical of wave reflection were recorded in only about 3% of the waves measured, but the evidence of

occasional exceptional pressure pulses is impressive. These exceptional cases show pressure intensities up to 100 psi, with durations of the order of 0.03 sec, for waves with deep water heights and lengths of the order of six and 150 ft., respectively. This investigation was not carried beyond the point of demonstrating the occurrence of exceptional pressure transients during wave breaking, but did serve to stimulate the model and analytical studies of Bagnold, as described in the next section.

B. Laboratory Investigations

Studies of breaking waves, with particular emphasis on the transient pressure impulse, were conducted by R. A. Bagnold in 1938.[8] These experiments were conducted for strictly limited wave and geometric parameters, as follows:

still water depth	18"
toe depth	4"
foreshore slope	1:6.35
wave height	10"

Waves were generated as a series of solitary waves, timed to allow each wave to travel to the barrier and reflect back to the generator before a new one was generated. Measurement was by means of a quartz crystal piezoelectric transducer, with output signal amplified and displayed on a cathode ray oscilloscope. Since particular attention was given the so-called "shock" pressures, the wave parameters were determined experimentally to yield consistent shocks.

Bagnold recorded pressure-peaks as high as 35 psi, and observed peaks estimated at 80 psi, but the magnitude of the pressure peaks varied greatly from wave to wave, which to all appearances were identical, and in 90% of the cases no pressure peak occurred at all. Additionally, Bagnold observed that the areas of his pressure-time records were nearly constant, hence his results may be summarized as observations of consistent values of impulse (or momentum change) per unit area, coupled with highly inconsistent or variable values of peak pressure.

Bagnold offers an explanation for the occurrence and magnitude of the peak pressures in terms of the compression of a thin air layer trapped between the barrier and the advancing wave front. Slight variations in the

shape and thickness of this air layer account for the variation in peak pressures, and on the basis of adiabatic compression of the air and an empirically-determined constant, the following formula is proposed for the maximum pressure rise:

$$(p_{max} - p_o) = 0.54\,\rho u^2 \frac{H}{D}$$

where

u = wave velocity at impact
H = wave height
D = air cushion thickness
ρ = mass density of water

Minikin[9] has attempted to overcome the weakness of this formula - the undetermined value of D - and as the result of an unclear analysis offers the following modification of Bagnold's formula:

$$p_{max} = 2.9\ d_1\left(1 + \frac{d_1}{D_1}\right)\ \frac{H}{L} \text{ tons per sq. ft}$$

where

d_1 = toe depth, ft
D_1 = depth at foot of foreshore slope, ft
L = wavelength, ft

This dynamic pressure is assumed to act at the SWL, and to diminish parabolically to zero at distance $\frac{H}{2}$ above and below this level. The Beach Erosion Board currently recommends[10] a slight modification or interpretation of this formula for the calculation of barrier forces in cases of breaking waves.

Ross[11] has conducted model investigations similar to those of Bagnold, but for a variety of foreshore slopes, wave heights and wave periods. Ross's results are similar to Bagnold's; measurements of impulse per unit area are consistent, and occasionally high intensity, short-duration pressure pulses are recorded. Finally, Ross notes that the design of structures must be somehow based on the total wave momentum which has to be reversed, and that the high intensity, short-duration pressure pulses are probably not structurally significant.

III. ANALYTICAL CONSIDERATIONS

A. Impulse-Momentum Relationships

In any investigation of dynamic forces the prime relationship is Newton's Second Law,

$$F = ma = m\frac{dv}{dt}$$

By integrating with respect to time, the law of impulse-momentum is derived:

$$\int_{t_1}^{t_2} Fdt = \int_{t_1}^{t_2} madt$$

$$\int_{t_1}^{t_2} Fdt = mv_2 - mv_1$$

The term on the left side of this equation is the impulse of the force F during the time interval from t_1 to t_2, and the right side of the equation expresses the change in momentum during this same time interval.

This form of Newton's Second Law is especially useful in impact problems, where it is difficult to evaluate the time-dependent force values, but where the gross kinematics of the system are apt to be more readily measured, thus providing at least means to evaluate the force-time integral, or impulse.

The situation of waves impinging on a barrier is of the nature of an impact problem. For the case where the waves are reflected from the barrier and a standing wave system is formed, hydrodynamic theory provides reasonably accurate analytic expressions for the kinematics of the system at every instant of time. This permits the impulse-momentum equation to be solved in terms of force as a function of time, or alternatively, to solve for the force directly from the basic form of the Second Law. In the case of waves breaking against a barrier, detailed information relating flow velocities as a function of time is not available, and

kinematic information is limited to the knowledge of the total momentum prior to impact and the fact that at some later time the horizontal component of momentum is reduced to zero and finally attains some negative value as the water is splashed back from the barrier face. The limited information restricts the analytical evaluation of the wave effect on the barrier to the calculation of the magnitude of the portion of the total impulse which occurs during the time interval from wave contact to the instant of zero horizontal flow. It is important to recognize that interpretation of the total impulse per wave cycle is not possible, since the terminal wave momentum is not equal and opposite to the initial value, but is less by some unknown amount as the result of energy dissipation in the breaking process. Thus the only change in wave momentum which can be calculated is from the initial state to the situation of zero horizontal component.

Recognizing the limited nature of analysis possible for the breaking wave problem, it is nonetheless valuable to calculate the initial wave momentum in terms of wave parameters. Waves which break on waterfront structures are characterized by definite values of height and period in deep water. However, breaking occurs only because the structures are located in relatively shallow water at the shore end of a shoaling region. It has been found that when wave trains advance from deep water into shoaling regions, their behavior is described most accurately by the so-called solitary wave theory[12] as the depth decreases to values comparable to wave height. Thus it may be expected that wave momentum for the situation under study will best be calculated on the basis of solitary wave theory. In substantiation of this approach, investigations of longshore currents in the surf zone[13] have been made in which experimental data checked well with theoretical values calculated from solitary wave momentum considerations.

Referring to Fig. 1, which defines the geometry and nomenclature for a solitary wave, the shaded area, Q, is the cross section of the volume of water which is advancing with the wave velocity, C. The momentum per wave per unit width is therefore,

$$U = \rho Q C \ .$$

From Ref. 12, the first approximation solitary wave theory of Boussinesq yields:

$$C = \sqrt{g(d + H)}$$

$$\Omega = 4d^2 \sqrt{\frac{H}{3d}}$$

Also, the higher approximation due to McCowan provides a value for the highest possible wave height in terms of the water depth, or in other words, a specification of breaking wave geometry:

$$\frac{H_b}{d_b} = 1/2 \tan(1 \text{ radian}) = 0.7788.$$

Combining, we obtain the expression for the momentum of a breaking solitary wave:

$$U_b = 55.5\, H_b^{5/2}$$

(H_b in ft, U_b in lb-sec/ft, fresh water)

It remains to express H_b in terms of the deep water wave parameters; such a relation is given in Ref. 12, derived on the usual refraction basis that energy is conserved over a width, S of wave crest between adjacent orthogonals:

$$\frac{H_b}{H_o} = \frac{1}{3.3 \sqrt[3]{H_o/L_o}} \sqrt[3]{S_o/S_b} \, .$$

For wave approach normal to the straight contour lines of a simple flat beach, as in the experimental study, this expression becomes:

$$\frac{H_b}{H_o} = \frac{1}{3.3 \sqrt[3]{H_o/L_o}} \, .$$

Since the momentum can now be expressed in terms of deep water wave height for given deep water wave steepness (H_o/L_o), it can also be expressed in terms of the wave height, H, at any intermediate depth, d, since H_o and H are connected by the equations derived from Airy wave theory for wave refraction, and numerical values have been tabulated for H_o/H as functions of d/L_o, as in Ref. 10.

B. Measurement of Impulsive Functions

The measurement of time-dependent functions always raises questions as to the effect of the dynamic characteristics of the measuring instrument on the output signal which is considered to represent the applied stimulus. Most types of force measuring instruments produce their output signal as the result of a mechanical displacement resulting from the applied force. Thus the deflections of simple spring balances are read directly to obtain the load quantity, and a common electrical force transducer, the wire strain gage, undergoes a change in resistance proportional to the load-induced elastic strain. Since instruments are designed to produce a linear relationship between the mechanical displacement and the final observed or recorded load indication, the over-all effect of instrument characteristics on load indication may be analyzed in terms of the instrument deflection.

Typical force measuring instruments may be considered to approximate closely a classical mechanical oscillator; a concentrated mass against which the force is applied, suspended from a fixed support by an elastic spring and a viscous damping dashpot. In many cases, the damping capacity may be small and can be ignored, especially in the analysis of instrument response to transient forces where only the first cycle of instrument response is important. As a first approximation, therefore, the amplitude response of a simple spring-mass system can be taken as representative of the behavior of an instrument system used to measure impulsive functions.

Impulsive loads can be classified in two main categories, step functions and impulse functions. A load, F_o, which is applied in zero time and is then maintained at that constant value is termed a step function. A load, F_i, which is applied in zero time, maintained for a short time interval t_o, and then removed in zero time is termed an impulse function.

The response of a simple oscillator with mass m, and spring constant, k, to these basic types of loads, expressed as ratios to the static deflections which would be produced by the same load values, are:

(1) Step Function:

$$\frac{x}{F_o/k} = \left(1 - \cos \sqrt{\frac{k}{m}}\, t\right)$$

(2) Impulse Function:

$$\frac{x}{F_i/k} = (1 - \cos\sqrt{\frac{k}{m}}\, t), \quad 0 < t < t_o$$

$$= 2 \sin 1/2\sqrt{\frac{k}{m}}\, t_o \sin \sqrt{\frac{k}{m}}\,(t - \frac{t_o}{2}), \quad t > t_o \ .$$

Note that for $t_o << \frac{2\pi}{\sqrt{k/m}}$,

$$\frac{x}{F_i/k} = t_o \sqrt{\frac{k}{m}} \sin \sqrt{\frac{k}{m}}\, t \ , \quad \text{approximately.}$$

In the case of the step function, the dynamic response is an unsymmetrical oscillation at the natural frequency of the system, $f = 1/2\pi \sqrt{k/m}$, with minimum displacement of zero and maximum displacement of double the static value. In the case of the impulse function, for the small values of t_o which characterize the case of practical interest, the response is a symmetrical oscillation with amplitude proportional to the product of impulse duration and system frequency.

Any suddenly applied and then relatively slowly changing function results in instrument response similar to that of the step function. For example, the response to a suddenly applied exponential decrement,

$F = F_o e^{-at}$ is;

$$\frac{x}{F_o/k} = \frac{1}{\frac{a^2}{k/m} + 1}\,(e^{-at} - \cos\sqrt{\frac{k}{m}}\, t) + \frac{\frac{a}{\sqrt{k/m}}}{\frac{a^2}{k/m} + 1} \sin\sqrt{\frac{k}{m}}\, t \ ,$$

where, for the values of a small compared with $\sqrt{k/m}$, the sine term is negligible and the coefficient of the first term is essentially unity and the remaining difference from step function response is the substitution of the exponential term in place of unity. As a numerical comparison, calculations show that for a value of $a/\sqrt{k/m} = 0.11$, corresponding to a falling-off of force to one-half its original value in a time interval equal to the

natural period of the system ($T = 1/f = 2\pi / \sqrt{k/m}$), the amplitude response of the first oscillation is 1.7 times the static deflection, F_o/k, as compared with the factor, 2, in the case of the step function.

Similarly, the response to the ideal impulse function is representative of the effect of actual short-duration impulses. Suppose an impulse with unknown force-time dependency, but with known total value, $\int F dt$, and of known short duration compared with the system period, $2\pi / \sqrt{k/m}$, is applied to the mass. During the short time duration little displacement can occur, hence the spring can exert no force on the mass. Then, by the impulse-momentum relation, the mass acquires a velocity,

$$v_o = \frac{\int F dt}{m}$$

The free response of a simple spring-mass system originally at rest when given an initial velocity is,

$$x = \frac{v_o}{\sqrt{k/m}} \sin \sqrt{\frac{k}{m}}\, t ,$$

hence, in this case,

$$x = \frac{F dt}{\sqrt{km}} \sin \sqrt{\frac{k}{m}}\, t$$

which is identical with the previous solution for the ideal case, as is seen by equating the total impulse in the two cases:

$$F_i t_o = \int F dt .$$

Obviously, a rigorous analysis of instrument response is only possible if the exact relationship between force and time is known. In the study of breaking waves, we can be guided only by certain general relationships. Thus, combining the observations of impulsive pressures due to Bagnold and Ross, and those of steady pressures due to Gaillard, we may expect the actual force-time history to consist of two components; (1) an impulse of very short duration (0.001 to 0.004 sec. for the scale of Bagnold's and the present experiments), and (2), a suddenly applied and relatively slowly decreasing function. If the measuring apparatus is

constructed with its natural period short enough so that the "steady" component decreases slowly in comparison, and yet the period is not so short that the impulsive component is of comparable duration, then we may make a valid approximate analysis on the basis of impulse and step function response.

By superposition of the previously given solutions, therefore, the response to the combined function is:

$$x = \frac{F_i}{k} \; 2 \sin \sqrt{\frac{k}{m}} \; \frac{t_o}{2} \quad \sin \sqrt{\frac{k}{m}} \left(t - \frac{t_o}{2} \right) +$$

$$\frac{F_o}{k} \left[1 - \cos \sqrt{\frac{k}{m}} \; (t - t_o) \right] \quad (t > t_o) \; .$$

The values of t corresponding to maximum and minimum values of the response are found by equating to zero the derivative of the above expression. These values of t are then substituted in the expression to obtain x_1 and x_2, the maximum and minimum values of the response.

The results of such an analysis are:

$$x_1 + x_2 = 2 \frac{F_o}{k}$$

$$|x_1| \; |x_2| \doteq \frac{1}{k^2} \left(\sqrt{\frac{k}{m}} \; F_i t_o \right)^2$$

where the approximation is valid for t_o small compared with $2\pi / \sqrt{k/m}$.

Now, the instrument record is read in terms of force units on the basis of a calibration. Thus, a calibrating load of N lbs., which produces a displacement $x_n = N/k$ of the sensing instrument, is represented by a deflection, n, of the recording pen or trace. The calibration, therefore, equates a record deflection, n, to a load, N, or its equivalent, kx_n. In relating instrument response to the recorded signal which is interpreted on the basis of a force calibration, therefore, it is the product k_x which must be considered.

Thus the algebraic sum of successive plus and minus peaks of the recorded signal is:

$$n_1 + n_2 = kx_1 + kx_2 = 2F_o \ .$$

Hence the magnitude, F_o, of the step function component is one-half the sum of the first positive and first negative peak values of the calibrated instrument response record.

The product of the absolute magnitudes of the first and second peak readings is:

$$|n_1| \ |n_2| = |kx_1| \ |kx_2| \doteq \left(\sqrt{\frac{k}{m}} F_i t_o \right)^2 .$$

Hence the square root of the product of the absolute values of the first plus and minus force peaks is equal to the product of the total impulse of the impulsive component and 2π times the natural frequency of the instrument system.

IV. EXPERIMENTAL PROGRAM

A. Technique

The principal apparatus used in this study was the three-component wave force balance developed for the previous reflecting wave study, Refs. 1 and 2. Modifications required for this study included:

(1) Provision of T-slot connections of the test barriers to the balance to facilitate adjustment for variable toe depths.

(2) Substitution of shop-fabricated force sensing cells of 1000-lb capacity for the original Statham cells of 150- and 200-lb capacity. These cells consist of heat treated stainless steel bars, with milled flat gage section approximately 3/8" wide x 0.080" thick, to which four Baldwin Type AB-7 gages are bonded. Two gages are bonded on each side, with one on each side parallel and one on each side transverse to the gage axis. By use of matched gages, and by connecting all four gages in a bridge circuit, excellent cancellations of bending strain and temperature drift were obtained. The over-all length and threaded attachment provision were made identical to the original Statham cells.

In addition, an experimental viscous damper was constructed and evaluated. This device consisted of a flexure-supported flat plate, connected to the thrust frame and mounted with small clearance (approximately 1/32") between two fixed plates. Fluids of various viscosities were injected

between the plates in the trials, but it was concluded that for the high natural frequency of the balance (approximately 40 cps) it was not feasible to construct an effective damper. Later, analytical considerations indicated that for the measurement of impulsive forces a damper is not desirable.

The Statham cells used in the earlier work provided sufficient signal voltage to drive the recording oscillograph galvanometers directly, but the 1000-lb cells were necessarily of lower sensitivity, and amplifiers were required. A Consolidated Engineering Company 1000-cycle carrier amplifier was used for this purpose. This unit operated indifferently, requiring frequent servicing and being responsible for much delay in the experimental program.

The channel and wave generator were the same as those used in the earlier work. False sloping bottoms were constructed of sheet metal with timber reinforcement near the end of the channel. The balance could then be set up with the barrier at any desired toe depth by positioning the balance assembly at the corresponding horizontal station along the run of the sloping bottom. The bottom was sealed to the side walls, and the barrier to the bottom and to the walls with flexible neoprene tape. Figure 2 shows a typical balance installation.

By providing for variable toe depths in the manner described, the water depth in the horizontal bottom portion of the channel was maintained at two feet. This permitted the use of a single wave generator crank arm - wave height calibration for a given wave period for all toe depths, and greatly facilitated the work. No attempt was made to measure wave heights at the barrier, since the unstable form of the waves at or near the breaking condition make such measurements of doubtful accuracy and because it was anticipated that any data obtained would be of greatest value when referred to deep water wave parameters. Accordingly, the wave generator calibration was used to specify the wave condition in the two-foot water depth, and these values were later converted to deep water conditions by standard methods.

Two auxiliary investigations were made in addition to the main effort devoted to wave force and moment measurements. First, a barium titanate piezo-electric pressure transducer and recording cathode ray oscilloscope

were used to measure the extremely short-duration pressure transients investigated by Bagnold and Ross. Second, stroboscopic photography was employed to investigate the kinematics of breaking waves. Attempts were made to record both the breaking wave profile changes near the barrier and the particle motion within the wave. The technique and apparatus employed were essentially identical with those described in Ref. 14.

B. Results

1. Breaking Parameters. When a wave train advances up an unobstructed sloping bottom, all waves will eventually become unstable and break. The relationship between the deep water wave steepness, H_o/L_o, and the depth of breaking can be predicted quite accurately, as discussed in Ref. 12. When the sloping bottom is terminated at a fixed still-water depth (toe depth) by a barrier, a different situation obtains. Because of the limitation on shoreward water volume imposed by the barrier, the backrush of each wave produces a draw-down or lowering of the water surface in the vicinity of the barrier which is much more pronounced than in the case of an unobstructed bottom. Thus the water depths encountered as a wave nears the barrier is not determined solely by the bottom geometry, but to a large degree by the characteristics of the preceding wave. As a result, waves higher than some limiting value will break to seaward of the barrier, and waves lower than another limiting value will not break at all, but will be reflected by the barrier and produce a standing wave system or "clapotis" to seaward. Between these limits, a range of wave heights all result in fairly well-defined breaking against the barrier.

Observations of limiting wave parameters for the reflecting and seaward breaking types of behaviors were made for each barrier-foreshore configuration. Figure 3 summarizes these observations in the form of plots of the parameter H_o/T^2 (which is essentially a measure of deep-water wave steepness, H_o/L_o, since $L_o = 5.12T^2$) vs. the parameter, d/T^2 (which is similarly proportional to the relative toe depth, d/L_o). The experimental data give good definition of the limiting curves which separate the three types of wave action.

Comparing the effect of barrier inclination, as shown by the two cases with 1:10 foreshore slope, shows little effect with respect to the criterion

for just breaking on the barrier, but indicates a somewhat smaller range of wave heights at each toe depth for which barrier breaking occurs in the case of the sloping barrier.

Comparing the effect of foreshore slope shows major influences of this factor. For the 1:3 slope, the influence of toe depth is minor, and the condition for barrier breaking is very nearly a function of deep water wave steepness only. With the 1:10 slope, linear relationships for the limits of both reflection and offshore breaking are found over the entire range of wave parameters studied. The slope of the curves in the 1:30 case are much steeper than those of the 1:10 cases in the lower range of height and depth parameters, while the reflection limit line approximates those for the 1:10 cases in the upper range of wave parameters. Thus waves of low deep water steepness can break in greater toe depths for the flatter slope, whereas for higher deep water steepness, the effect of slope becomes of less importance.

2. Impulse - Momentum Comparisons. It has been pointed out that available theories make possible the calculation of the momentum of a breaking wave in terms of either deep water wave height or the wave height in a known depth. The initial momentum is numerically equal to the change in horizontal component of momentum up to the time at which all forward motion of the water has been brought to rest by the barrier, and reverse motion begins. This momentum change is therefore equal to the horizontal thrust impulse which is resisted by the barrier reactions during the same time interval. If this time interval can be determined, therefore, it is possible to determine experimentally the validity of the momentum theory by means of impulse measurements.

Inspection of the force-time data recordings reveals an important characteristic. In all cases of waves breaking on the barrier, the force-time curve shows first the gradual lowering due to draw-down, next the transient associated with an impulsively applied load, next a fairly rapid decrease followed by a smooth rise and a final decrease to fair into the next wave record. These characteristics are illustrated by typical records, Fig. 4. Now, in the case of wave reflection, the force-time record is a smooth, more-or-less sinusoidal curve, and it is readily shown analytically that the maximum force occurs at the instant when the flow has been

brought to rest. By analogy, therefore, it is assumed that in the case of breaking waves the time at which the force reaches its second maximum during the smooth part of its curve is the instant of zero horizontal momentum.

Impulse data were obtained for a wide range of wave heights and toe depths for each wave period in all except the 1:3 slope case. The force-time curves were traced directly from the oscillograph data, the transient portion being faired in the process, and the areas which are proportional to the impulse, measured by planimetering from the start of the transient initial force rise to the second peak. A sample record is shown in Fig. 4. These data are presented in Fig. 5, where it is observed that in most cases the points corresponding to barrier breaking are in reasonable agreement with the solitary wave momentum theory. The points which correspond to offshore breaking are in most cases lower than the theory curve, indicating the energy loss in the plunging type of break to seaward of the barrier.

The verification of the momentum theory is an important result of these studies, since it permits the use of this theory in evaluating other data, as will be seen in the following sections.

3. Force Measurements. The considerations outlined in the discussion of theory have guided the evaluation of forces in this investigation. It is believed that the initial amplitude of the suddenly-applied but non-impulsive component of the breaking wave force is the significant quantity from the standpoint of structural design. Therefore, in cases where the presence of an initial impulse is indicated by a sine-component of the force record, the significant force, F, is calculated as one-half the algebraic sum of the first positive and first negative peaks of the record. In cases where no impulsive component is indicated, the records are "faired" to reconstruct the assumed suddenly applied load function; and the maximum value of the faired curve is read as F. The zero level of the force records is taken at the point of maximum draw-down, hence the force values represent the loading on the seaward face in excess of any hydrostatic component remaining at maximum draw-down. For most values of d/T^2 and H_o/T^2 which result in major forces, the toe of the barrier is nearly dry at maximum draw-down, hence any small hydrostatic contribution to the total force

on the seaward face can be ignored.

In all experimental runs data were recorded continuously for six to 10 wave periods. Considerations of wave velocity and channel length indicated the number of wave breaking sequences which could be assumed free of spurious reflection contributions from the wave machine. Measurements were confined to these initial records, but in many cases it was observed that even these steady-state records were not nearly identical. The procedure adopted in such cases was to record data for one "exceptional" and one "typical" record. (It may be mentioned here that subsequent analysis showed most exceptional data to differ chiefly in magnitude of impulsive component, while the amplitude, F, of the suddenly applied components did not usually differ greatly.) Additionally, experimental runs were made in triplicate for all wave heights which resulted in barrier breaking, and all such data were read, hence as many as six data points may be presented for a single wave and barrier situation.

Figures 6 are plots of force, F, as defined above vs. wave height in the constant-depth portion of the channel. These plots separate only the effect of barrier and foreshore geometry and wave period, and each such plot includes all values of barrier toe depths which were run. It is observed that the data of these plots may be bounded by upper limit curves, representing the functions

$$F = \frac{U_b}{\Delta t}$$

where U_b is the calculated breaking solitary wave momentum for the given wave heights, and the time interval Δt, is specified in terms of the wave period, T. These upper limit curves may therefore be considered as empirical relations between calculated momentum change and maximum effective force, F.

In Figs. 7, 8, 9 and 10 the same data are presented in dimensionless form to facilitate the interpretation of these model results in prototype terms, and the effect of toe depth, which is masked in the previous figures, is emphasized. The ordinate, $F\,T/2\,U_b$, of these semi-logarithmic plots expresses the ratio of an impulse of amplitude F, the measured force, and duration T/2, one-half the wave period, to the computed wave momentum.

The ordinate, H_o/T^2, is in the form of deep-water wave steepness. By separating the data into groups with narrow ranges of the relative toe depth parameter, d/T^2, the relationship between maximum effective force and computed momentum is more clearly seen. Thus, it is observed that the empirical limit curves which have been fitted to these plots decrease in every case from a relative high value at the minimum wave steepnesses for breaking to lower values at increasing wave steepness.

Studying first the effect of toe depth, it is seen that this has little effect on the maximum value of the force-momentum parameter at comparable values of wave steepness, namely those corresponding to the onset of wave breaking.

What these plots emphasize most strongly is the effect of barrier and foreshore geometry. Comparison of the data for the 1:30 slope - vertical barrier, 1:10 slope-vertical barrier and 1:10 slope - 30° barrier shows maximum values of $FT/2U_b$ of approximately 13, 10 and 5, respectively. Thus, for fixed values of wave period, flattening the slope from 1:10 to 1:30 results in 30% greater maximum effective forces against a vertical barrier, and inclining the barrier 30° shoreward halves the forces.

The 1:3 slope case represents a considerably different situation from the other cases studied. Since breaking occurs only for the highest range of wave steepness, only few data could be obtained. The results are most similar to those for the 30° sloping barrier, the maximum values of the force-momentum parameter being about the same in both cases.

4. Moment Measurements. Recorded values of moment about the balance axis were read in the same manner as described for the force data. These moment data were converted to values of moment about the barrier toe and to center of pressure distance above the toe by methods described in Ref. 2. The results are separated in groups by d/T^2, and presented in the form of dimensionless plots of $c.p./H_o$, the ratio of center of pressure distance above the toe to the deep-water wave height, vs. H_o/T^2, the deep-water wave steepness parameter, in Figs. 11, 12, 13 and 14.

The limit curves on these plots have been faired in by eye and establish empirical relationships which may be useful in design. These limit

curves indicate that the onset of breaking (at minimum values of H_o/T^2) is associated with the highest position of the center of pressure, as well as the highest force values as noted previously. Thus the overturning stability of a structure is most severely taxed at values of wave parameters and toe depths which combine to define the breaking line, as in Fig. 3.

5. "Shock" Impulse Measurements. As derived earlier in the discussion of theory, the magnitude of any short-duration impulse superposed on the longer-term force function is approximately proportional to the square root of the absolute magnitude of the first positive and first negative peak of the recorded force-time history:

$$\sqrt{F_1 F_2} = 2\pi fI$$

Evidence of an impulsive component of the applied force was observed only in the cases with 1:10 foreshore slope, and the absence of such a component was a notable feature of the 1:30 slope case.

The data are presented as plots of I/U_b, the ratio of measured shock impulse to computed wave momentum, vs. H_o/T^2 in Figs. 15 and 16. In the case of the vertical bulkhead, there is considerable scatter in the data, as would be expected in view of Bagnold's and Ross's experiments, with the indication of a trend to higher ratios - up to a maximum of about 0.10 - with increasing relative toe depth. Waves breaking on the 30^o barrier resulted in much fewer and weaker impulses than in the case of the vertical barrier, the maximum intensity being but 2% of the computed momentum change.

These results are in general agreement with those of Ross and Bagnold. Thus, Ross notes values of 0.02 psi-sec for the integral values of his recorded pressure-time curves with 7-in. waves. With this value of wave height:

$$U_b = 55.5\, H_b^{5/2} = 14.4 \text{ lb-sec/ft}$$

and from the data reported herein:

$$I \doteq 0.07\, U_b = 1.01 \text{ lb-sec/ft} .$$

Now:

$$I = 12h \int p\,dt \text{ lb-sec/ft}$$

where $\int pdt$ is in psi-sec and h is the height in inches of the area over which the pressure acts.

Then, $$\int pdt = \frac{0.084}{h} \text{ psi-sec}$$

$$= 0.021 \text{ for } h = 4" .$$

This value of vertical distance over which the pressure acts appears about right on the basis of Bagnold's and Ross's work.

As mentioned earlier, a brief investigation of shock pressures was conducted in a manner similar to that employed by Ross and Bagnold. This program was undertaken before Ross's results were available, and was prompted by some uncertainties regarding Bagnold's work, especially his instrument calibrating procedure. Sufficient measurements were made to corroborate the main features of the earlier work, but no attempt was made to perform a systematic analysis of the pressure-aspect of the shock impulse problem.

6. Breaking Wave Kinematics. It has been pointed out that a detailed analytical investigation of breaking wave forces requires knowledge of the flow, or velocity-time relationships, during the breaking process. In the absence of such information, certain approximations have been used - such as the calculation of momentum from solitary wave theory - but the obvious physical differences between the actual case and the approximate models renders these makeshifts rather unconvincing. Thus, the breaking solitary wave is symmetrical about the crest, whereas a real breaking wave, whether on beach or barrier, is highly unsymmetrical.

Biesel[15] suggests an extension of classical wave theory for use in analyzing wave kinematics over sloping bottoms. This theory yields wave profiles at the breaking point which appear very real, and for that reason calculations for some typical cases were carried out using his method. These calculations showed, however, that agreement between the theory and reality is mainly qualitative. Thus, although the calculated profiles appeared "real", the calculated wave velocities were much lower than experimental measurements.

In this situation, some time was spent in an investigation of the

possibility of directly measiring detailed kinematic relations in a breaking wave. Stroboscopic techniques, as described in Ref. 14, were employed to record both wave profile and particle motion. The extreme difficulty of recording the motion of neutral density particles during the violent agitation of the breaking process prevented the attainment of quantitatively useful results in the time available. However, this experience resulted in the conviction that this technique is capable of refinement and improvement to the point where much valuable data could be obtained.

Figure 17 illustrates some typical results of this program. In Fig. 17a, the advancing wave profile is recorded, and the typical steepening front face, resulting in a nearly vertical water face at barrier impact is clearly shown. In Fig. 17b, the motion of particles is easily followed up to the point where they are obscured by splash and spray.

V. CONCLUSIONS

The following conclusions may be drawn from this study and applied in the design of structures subjected to breaking waves.

(1) The force acting on a plane barrier as the result of wave breaking is characterized by a suddenly applied (essentially in zero time), relatively slowly decreasing component, which may be accompanied by a very short duration impulsive component. The maximum value of the short-duration impulse does not appear to exceed, and is usually much less than, 10% of the impulse of the persistent component from the time of wave contact to the time of wave momentum reversal.

(2) The maximum (initial) value of the suddenly applied persistent force component is considered a significant quantity upon which to base structural design. In this regard, it is important to take into account the rapid-loading nature of this force when selecting a factor of safety for design purposes.

(3) Solitary wave theory provides a reasonably accurate means for calculating the momentum of a breaking wave. The momentum calculated on this basis is equal to the impulse of the force experienced

by a barrier from the time of initial wave contact to the time of wave momentum reversal.

(4) The experimentally obtained relationships presented herein provide numerical values from which the maximum effective breaking wave force and moment can be calculated for given wave and barrier conditions. The values so calculated are in excess of those obtained by the Beach Erosion Board adaptation of Minikin's method.

(5) Inclining the barrier 30° shoreward from the vertical appears to halve the forces which would be experienced by a vertical barrier. It is believed that this effect is an important subject for further study.

VI. REFERENCES

1. Carr, J. H. (1953) "Wave Forces on Plane Barriers", California Institute of Technology, Hydrodynamics Laboratory Report No. E-11.1, October 1953.

2. Carr, J. H. (1954) "Wave Forces on Curved and Stepped Barriers", California Institute of Technology, Hydrodynamics Laboratory Report No. E-11.2, June 1954.

3. Gaillard, D. D. (1935) "Wave Action in Relation to Engineering Structures", The Engineer School, Fort Belvoir, Va.

4. Molitor, D. A. (1935) "Wave Pressures on Seawalls and Breakwaters", Trans. ASCE, Vol. 100.

5. Munk, W. H. (1948) "Wave Action on Structures", Petroleum Technology, Vol. 11, No. 2, March 1948.

6. Mueller, L. A., Knutson, H. A. and Koch, A. A. (1953) "Some Dynamic Aspects in the Design of Marine Structures on the Great Lakes", Proc. of Fourth Conf. on Coastal Engineering, October 1953.

7. Rouville, M. A., Besson, P. and Petry, P. (1938) "Etat Actuel des Etudes Internationales sur les Efforts dus aux Lames, Ann. Ponts et Claussees, Vol. 108 (11).

8. Bagnold, R. A. (1939) "Interim Report on Wave-Pressure Research", Journal Institution of Civil Engineers, Vol. 12, June 1939.

9. Minikin, R. R. (1950) "Winds, Waves and Maritime Structures", Chas. Griffen and Co., Ltd., London.

10. Corps of Engineers, Dept. of the Army (1953) "Bulletin of the Beach Erosion Board," Special Issue No. 2 (Preliminary), March, 1953.

11. Ross, C. W. (1953) "Shock Pressure of Breaking Waves", Proc. of Fourth Conf. on Coastal Engineering, October, 1953.

12. Munk, W. H. (1949) "The Solitary Wave Theory and its Application to Surf Problems", Annals of the N. Y. Academy of Sci., Vol. 51, Art. 3, May 1949.

13. Putnam, J. A., Munk, W. H, and Traylor, M. A., (1949) "The Prediction of Longshore Currents", Trans. Am. Geophysical Union, Vol. 30, No. 3, June 1949.

14. Elliott, J. G. (1953) "Interim Report", California Institute of Technology, Hydrodynamics Lab., Hydraulic Structures Division, July 1953.

15. Biesel, F. (1951) "Study of Wave Propagation in Water of Gradually Varying Depth", National Bureau of Standards Circular 521.

APPENDIX

COMPARISON OF CALCULATED WAVE FORCES

As an illustration of the application of the data presented in this report to the calculation of forces and moments in a typical prototype situation, and to emphasize the difference between the results of such calculations and those obtained by application of the Beach Erosion Board - Minikin procedure. The following calculations are presented:

1. Problem:

   A vertical barrier located in 8-ft water depth on a 1:10 sloping coast. Deep-water waves of 6-ft height and 9-sec period are occurring offshore of the barrier.

2. Forces on the Seaward Side, and Resulting Moment by the Method of Report E-11.3:

   (a) $L_o = 5.12\ T^2 = 415$ ft

   (b) $\frac{H_o}{L_o} = 0.0145$

   (c) $H_b = H_o \frac{1}{3.3\ \sqrt[3]{H_o/L_o}} = 7.5$ ft

   (d) $U_b = 55.5\ H_b^{5/2} = 8550$ lb - sec/ft (fresh water)

   (e) $\frac{d}{T^2} = 0.099$

   (f) $\frac{H_o}{T^2} = 0.074$

   (g) From Fig. 7c, $\frac{F\,T}{2U_b} \doteq 10$

   (h) $F = 19,000$ lbs/ft (fresh water)

(i) From Fig. 11c, $\frac{c.p.}{H_o} \doteq 2.5$

(j) $M = F_o \cdot c.p. = 285,000$ ft-lbs/ft (fresh water).

3. Forces on Seaward Side, and Resulting Moment by Beach Erosion Board - Minikin Method (Ref. 10):

(a) $\frac{d}{L_o} = 0.0193$, $\frac{d}{L_d} = 0.0566$, $\frac{H}{H_o} = 1.24$ (Table D-1)

(b) $D = d + L_d S = 22.2$ ft

(c) $\frac{D}{L_o} = 0.535$, $\frac{D}{L_D} = 0.0977$ (Table D-1)

(d) $L_D = 227$ ft

(e) $p_m = \frac{101\ wH}{L_D}\left(\frac{d}{D}\right) = (D + d)$, 2240 lbs/ft^2

(f) $p_d = w(d + \frac{H}{2}) = 731$ lbs/ft^2

(g) $R = \frac{p_m H}{3} + \frac{1}{2} p_d (d + \frac{H}{2})$

$= 5550 + 4290 = 9840$ lbs/ft (sea water)

(h) $M = R_p \cdot d + R_d \cdot \frac{d + \frac{H}{2}}{3}$

$= 61,100$ ft - lbs/ft (sea water) .

Thus, the results of this study indicate forces twice as great, and moments four times as great, as the quantities computed by use of the Beach Erosion Board - Minikin method.

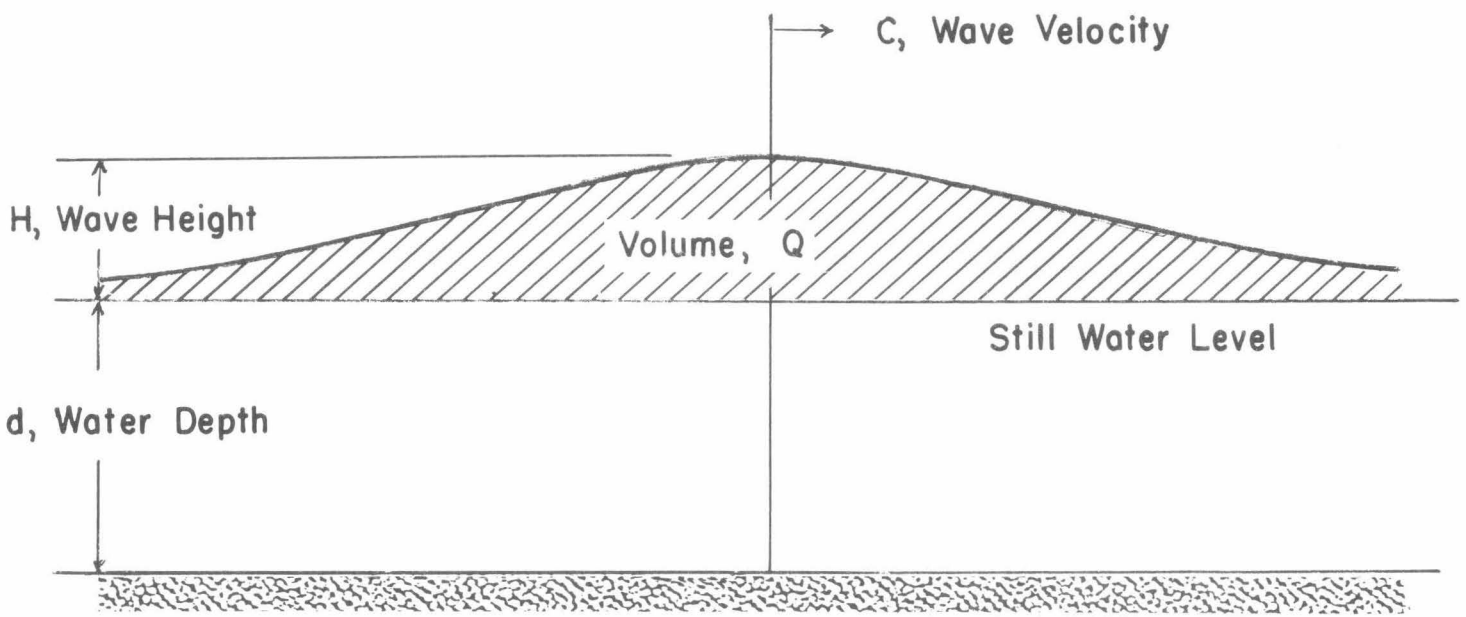

Fig. 1 - Solitary wave notation

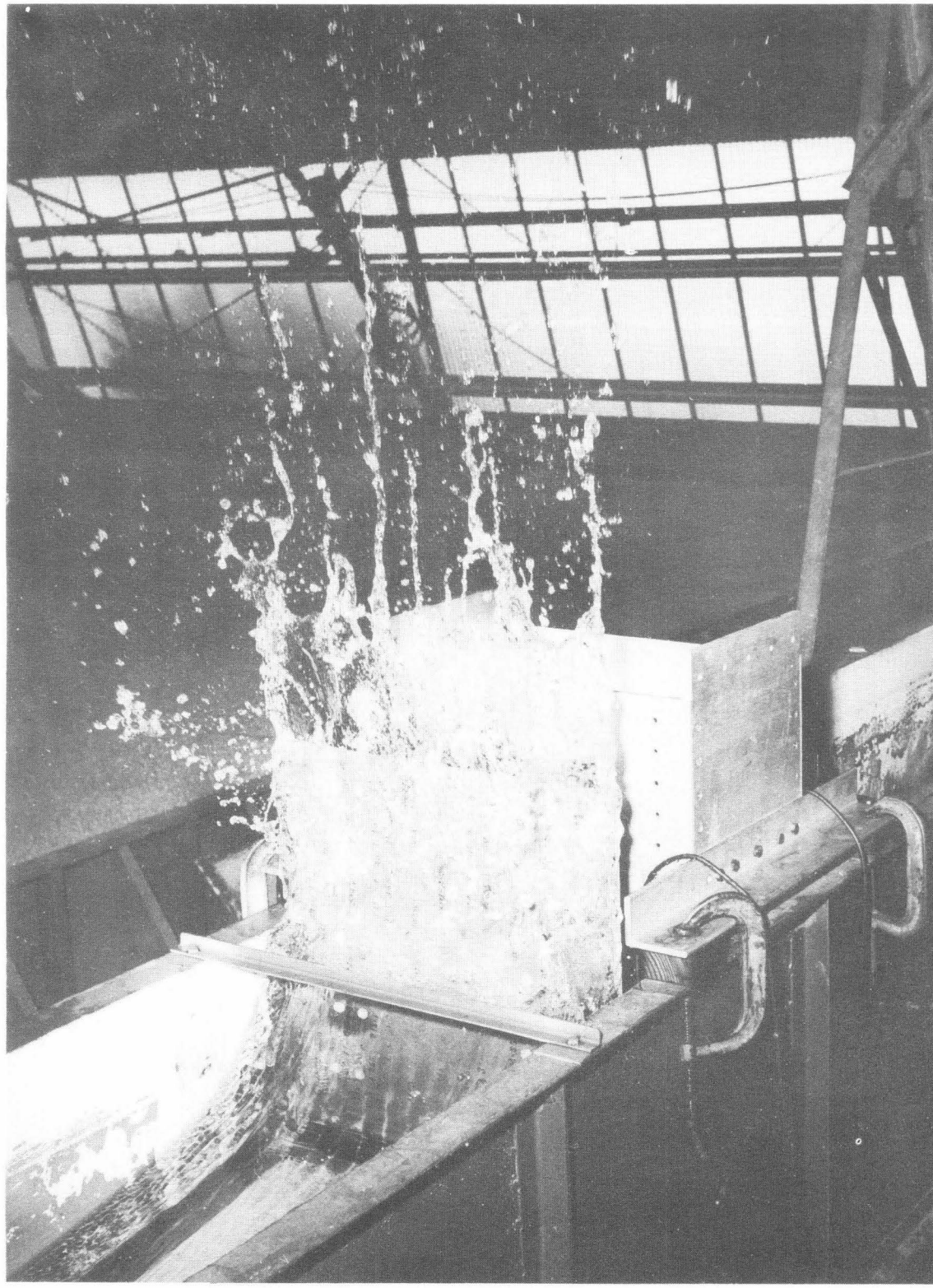

Fig. 2 - Typical balance installation

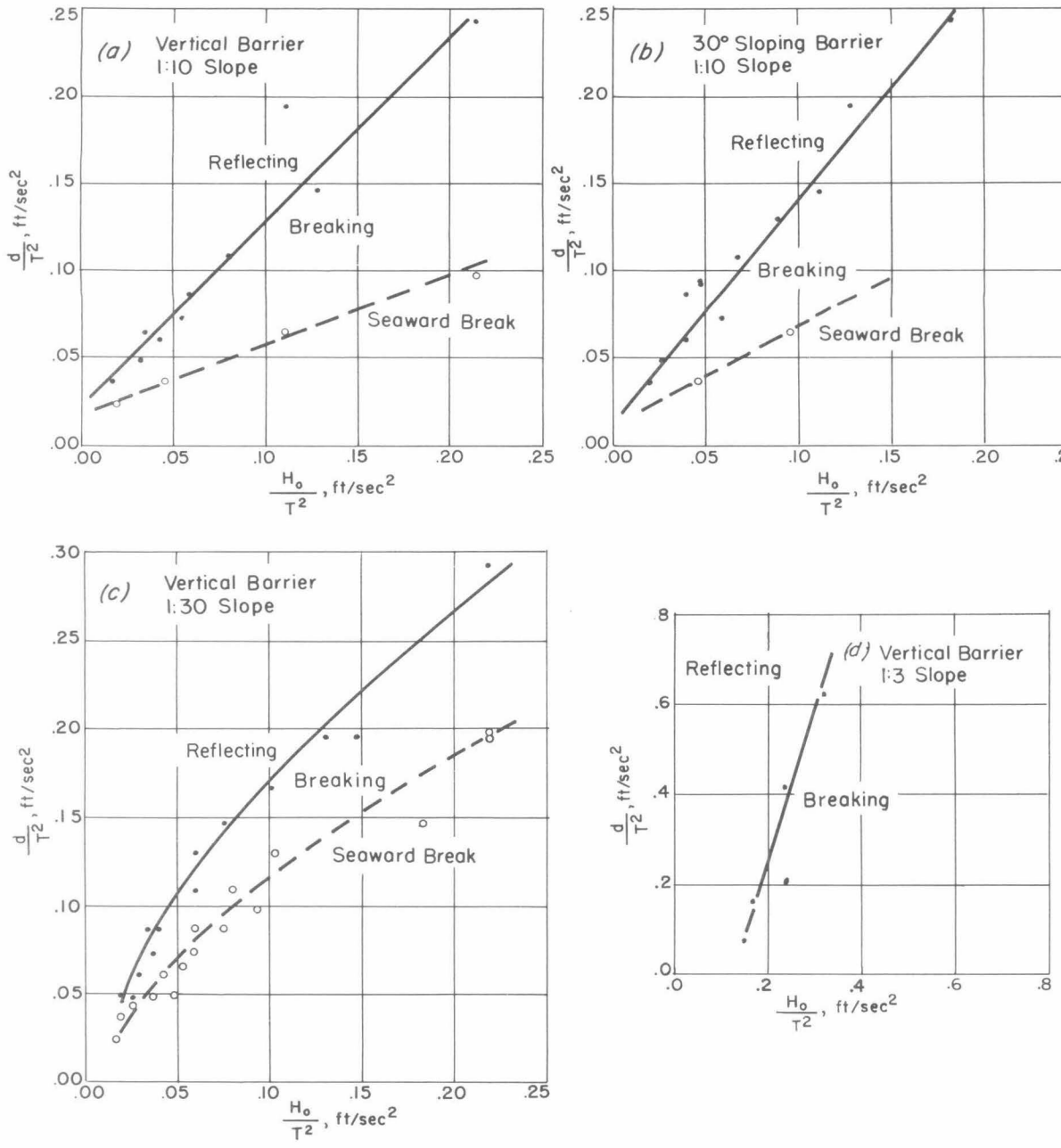

Fig. 3 - Wave breaking parameters

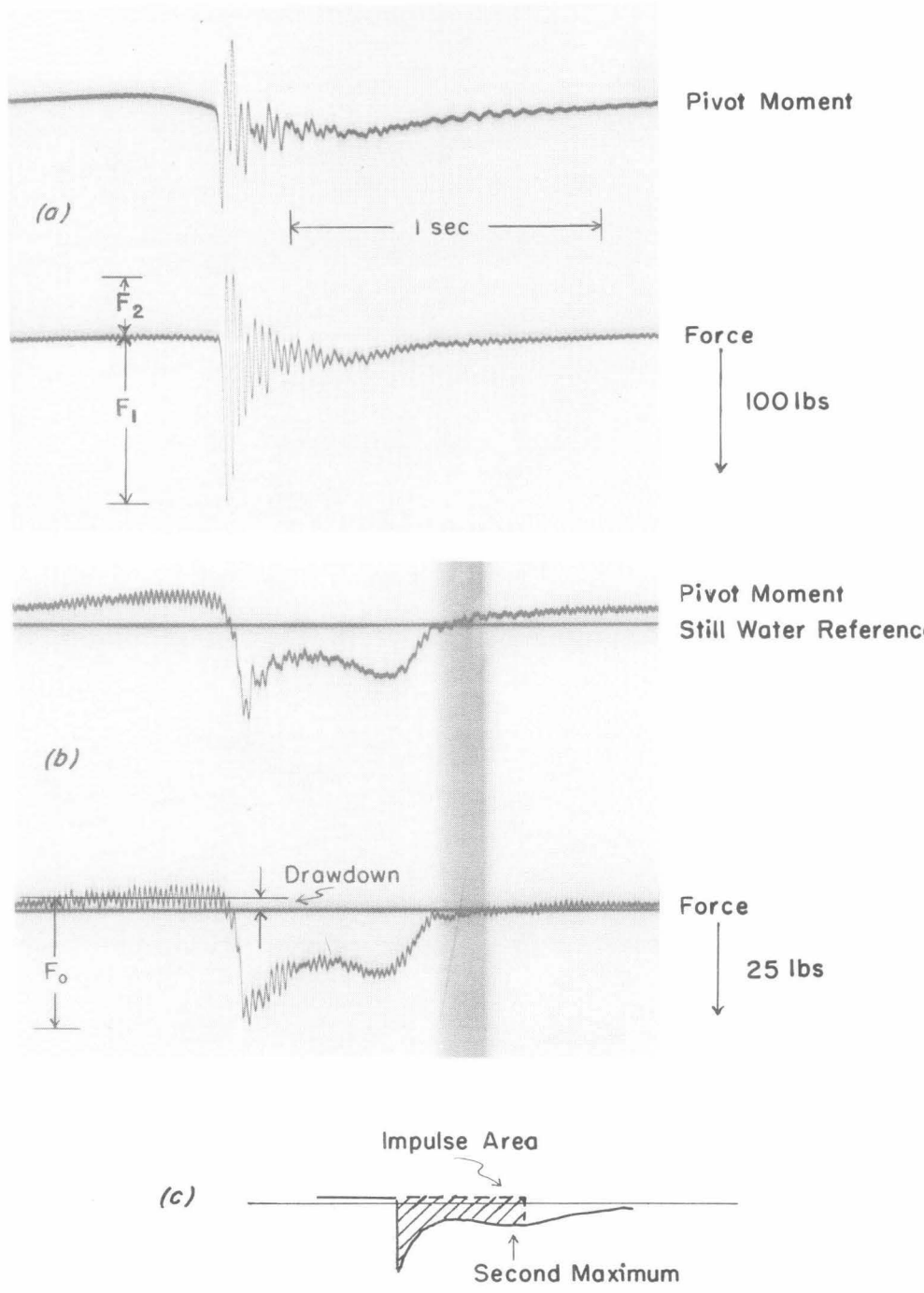

Fig. 4 - Typical balance records

(a) Vertical barrier, 1:10 slope, $\frac{H_o}{T^2} = .073$, $\frac{d}{T^2} = .087$

(b) Vertical barrier, 1:30 slope, $\frac{H_o}{T^2} = .059$, $\frac{d}{T^2} = .087$

(c) Faired force-time record (a) for impulse measurement

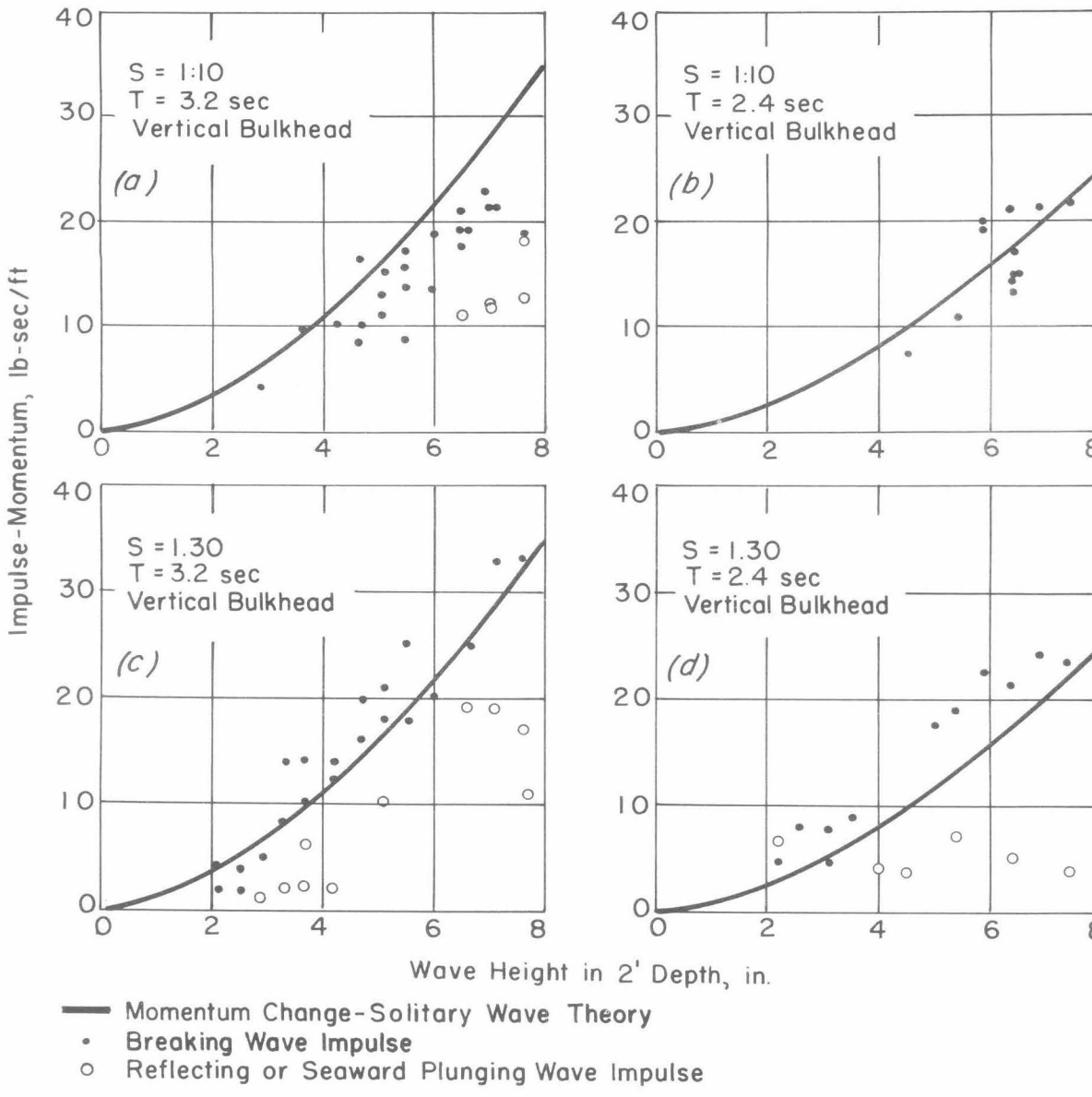

Fig. 5 - Comparison of measured impulse and calculated momentum change

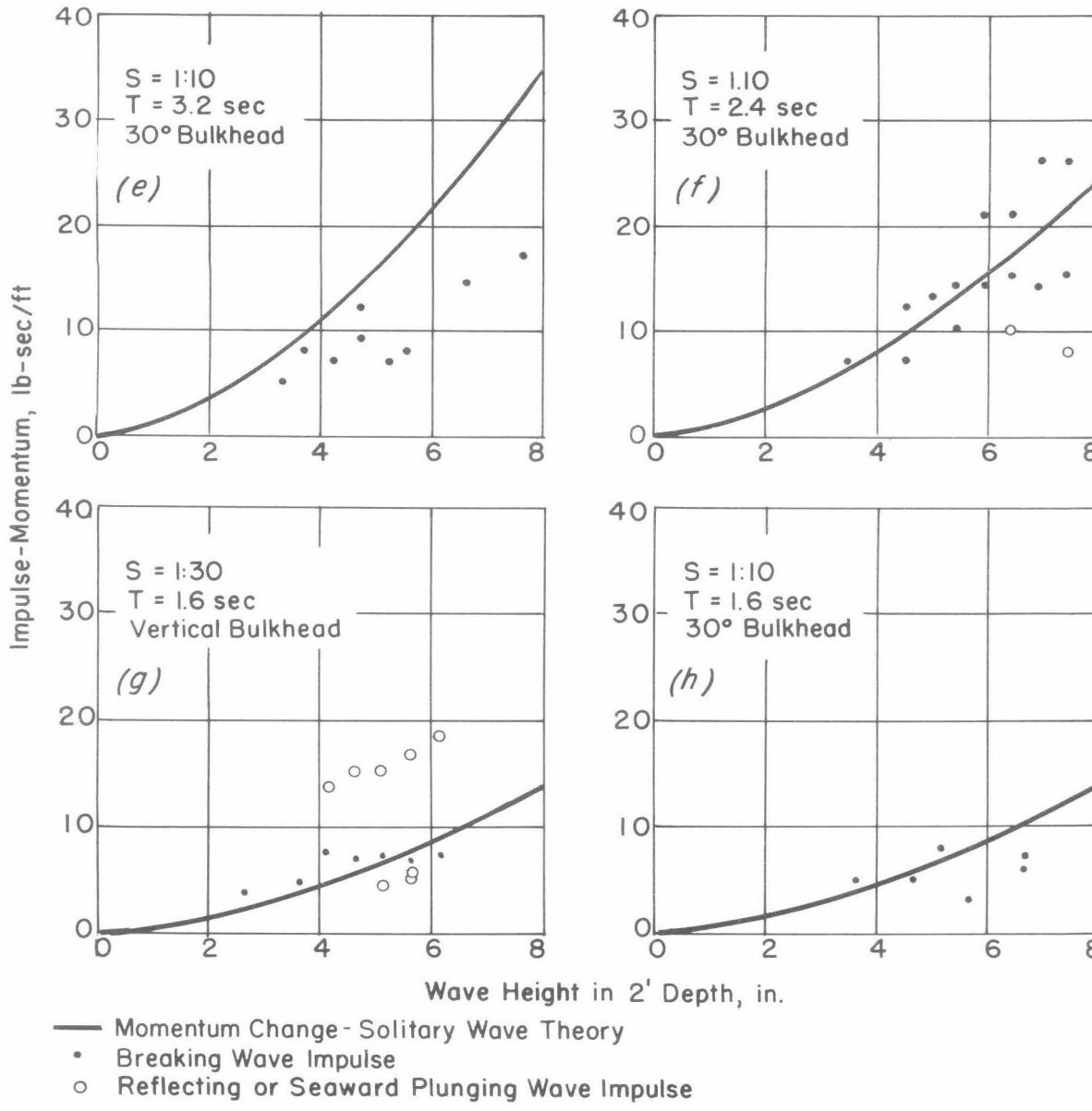

Fig. 5 (cont) - Comparison of measured impulse and calculated momentum change

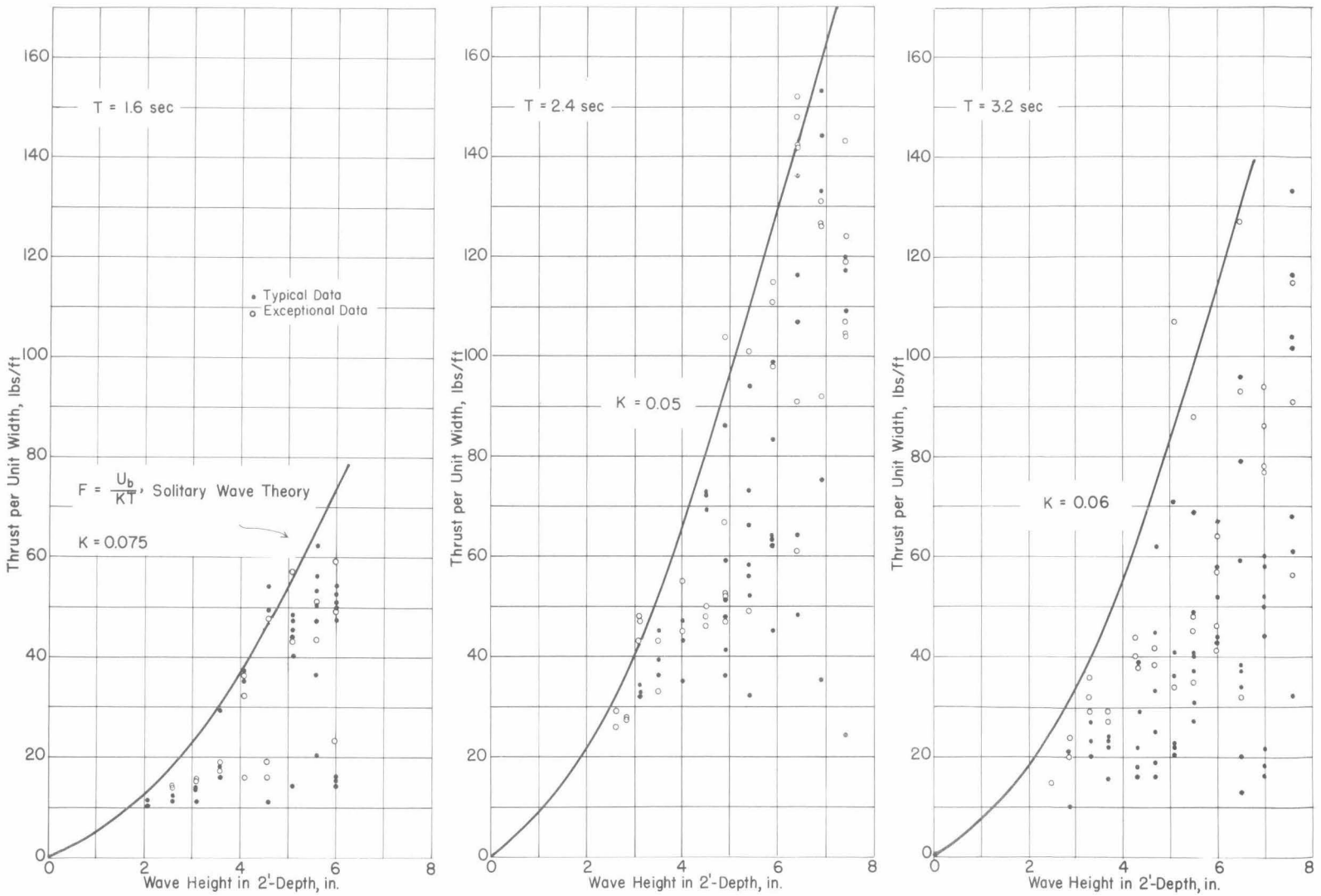

Fig. 6a - Measured force data, vertical barrier, 1:10 slope

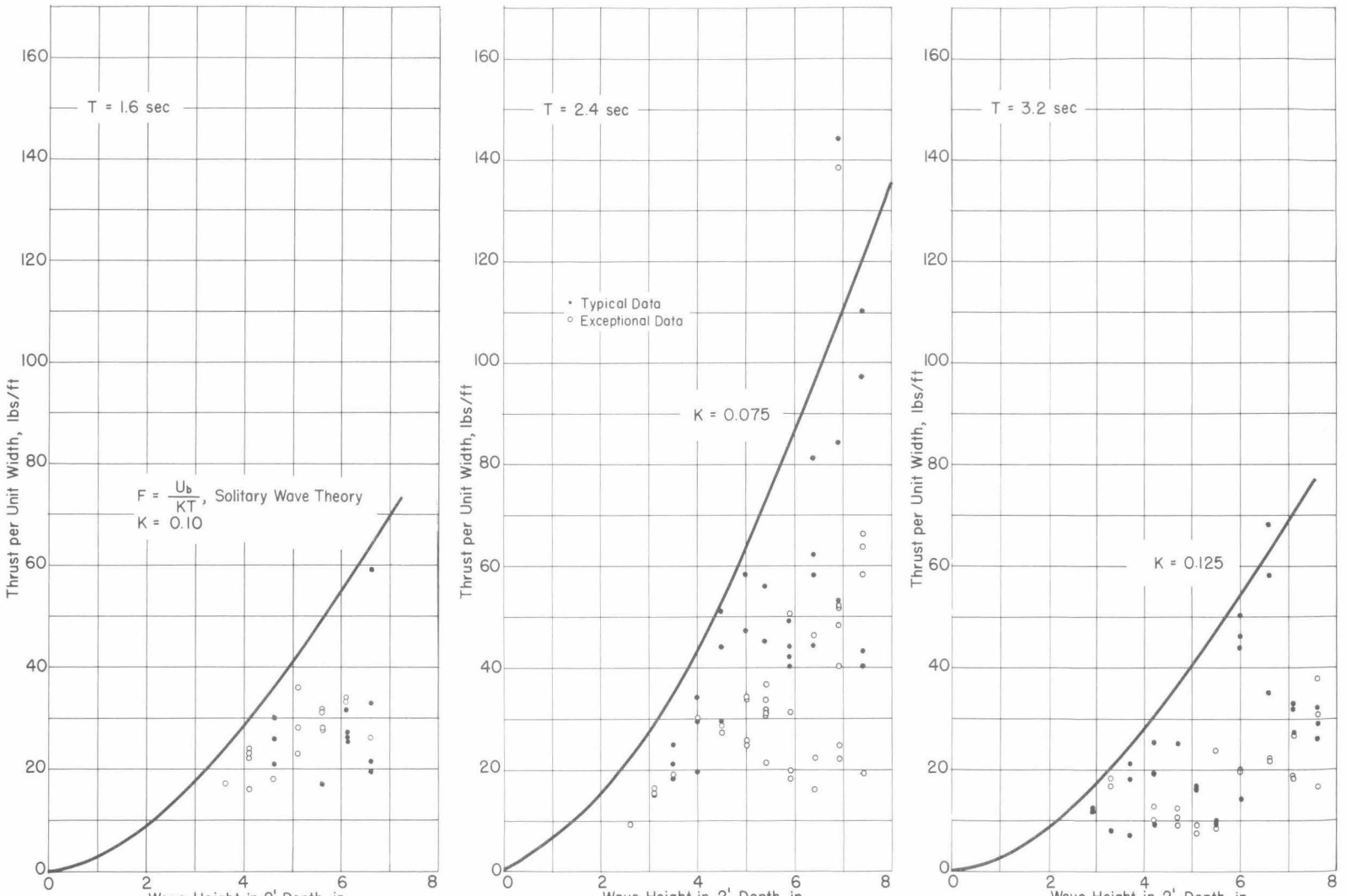

Fig. 6b - Measured force data, 30^{o} sloping barrier, 1:10 slope

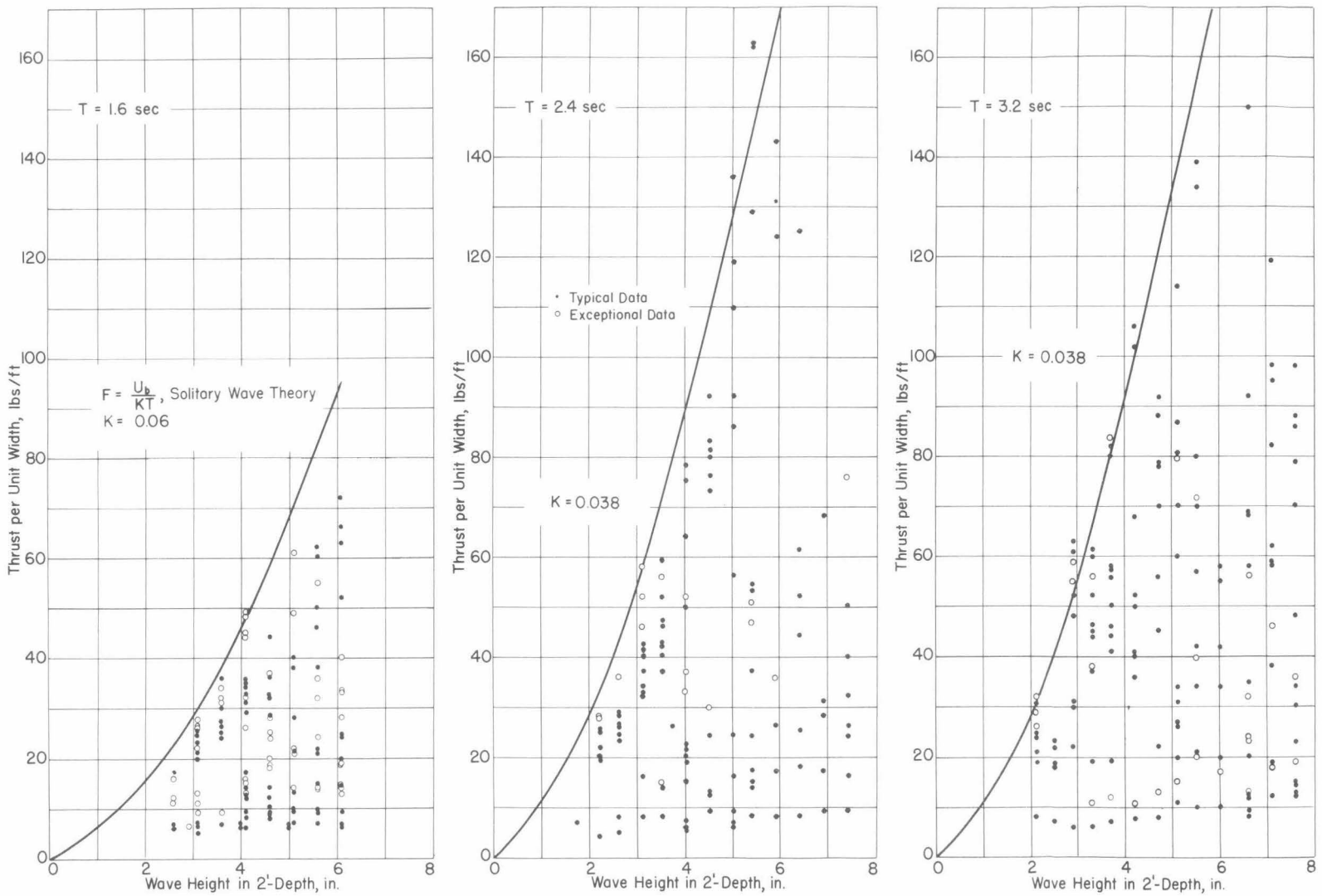

Fig. 6c - Measured force data, vertical barrier, 1:30 slope

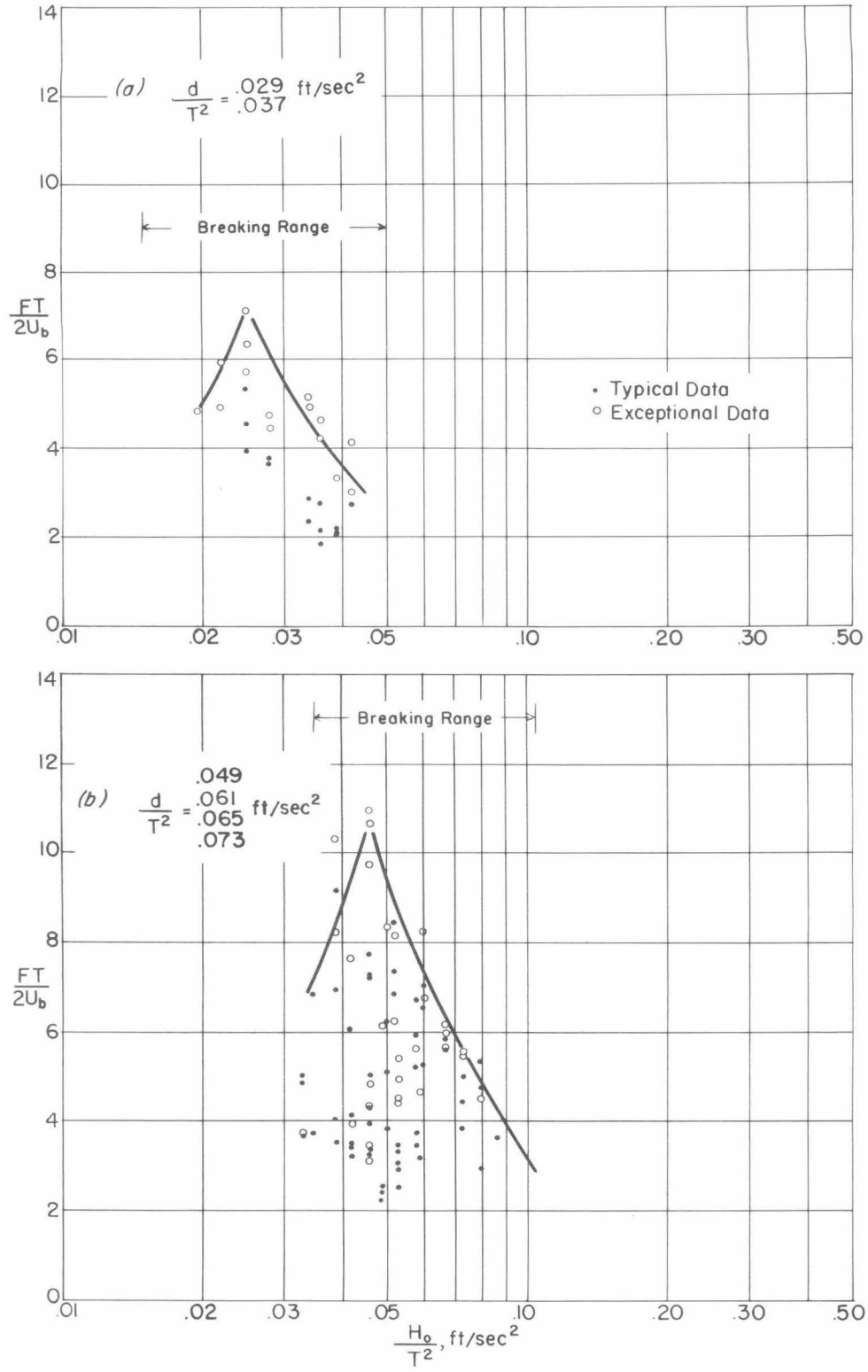

Fig. 7 - Dimensionless representation of force data, vertical barrier, 1:10 slope

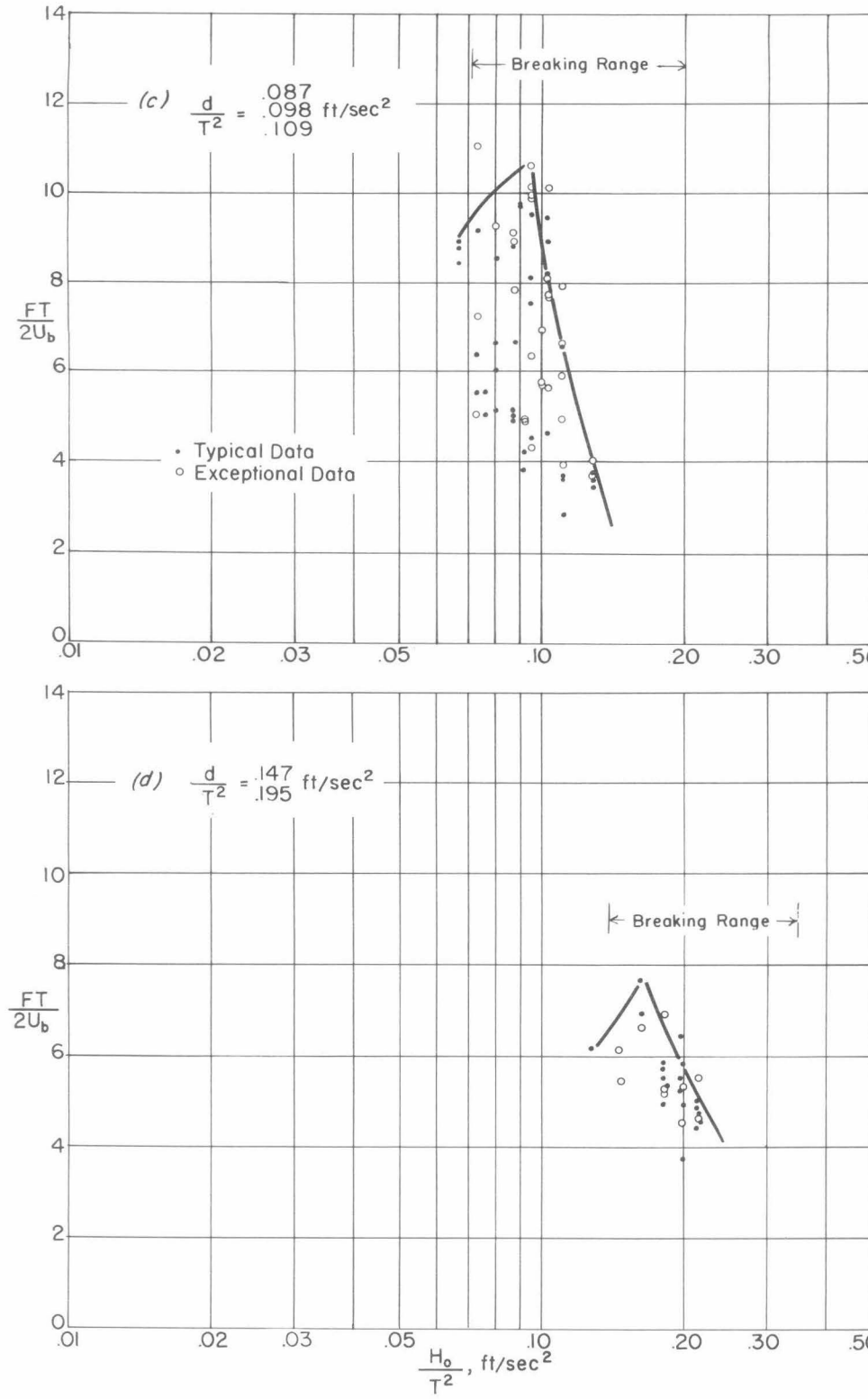

Fig. 7 (cont) - Dimensionless representation of force data, vertical barrier, 1:10 slope

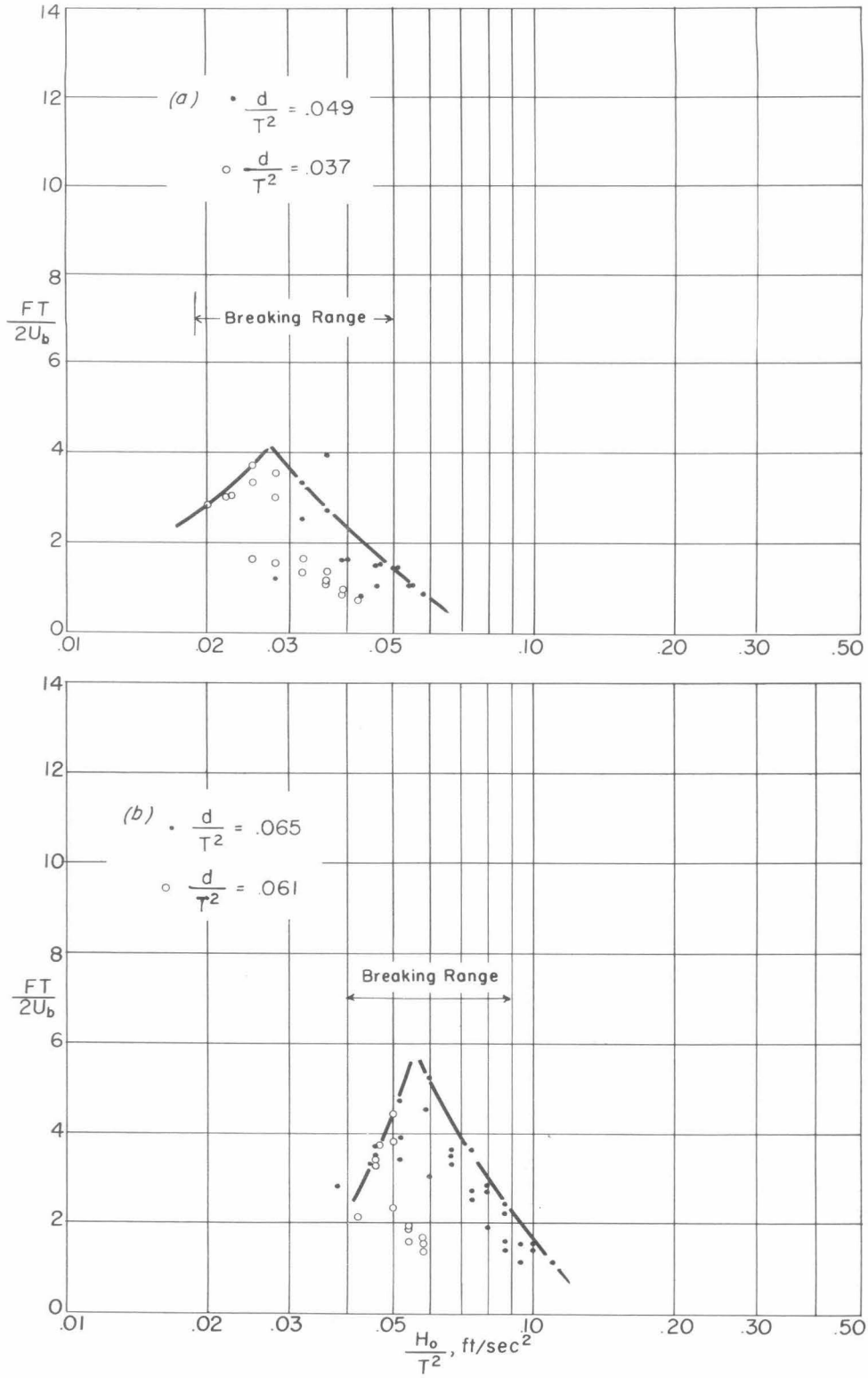

Fig. 8 - Dimensionless representation of force data, 30^{o} sloping barrier, 1:10 slope

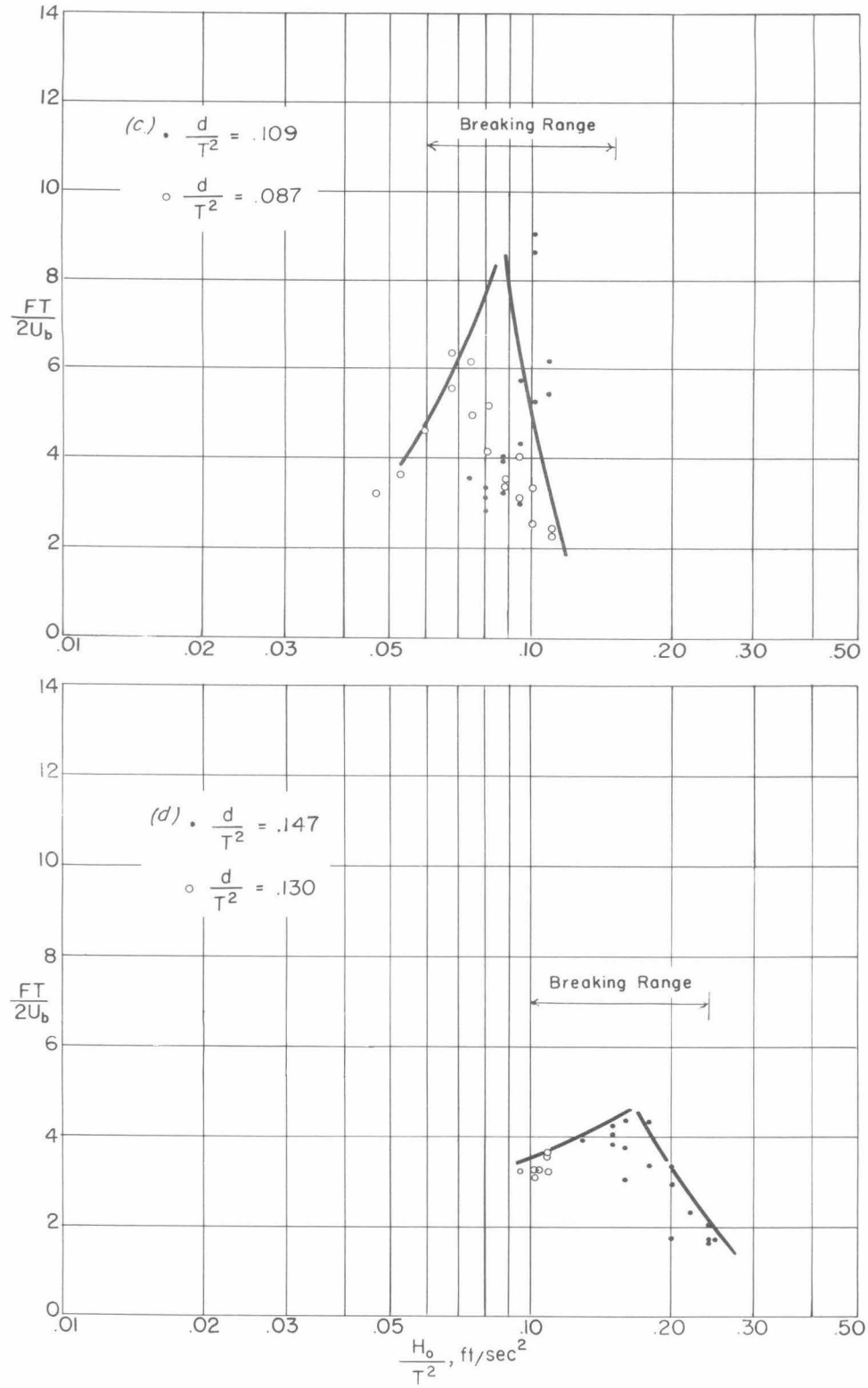

Fig. 8 (cont) - Dimensionless representation of force data, 30° sloping barrier, 1:10 slope

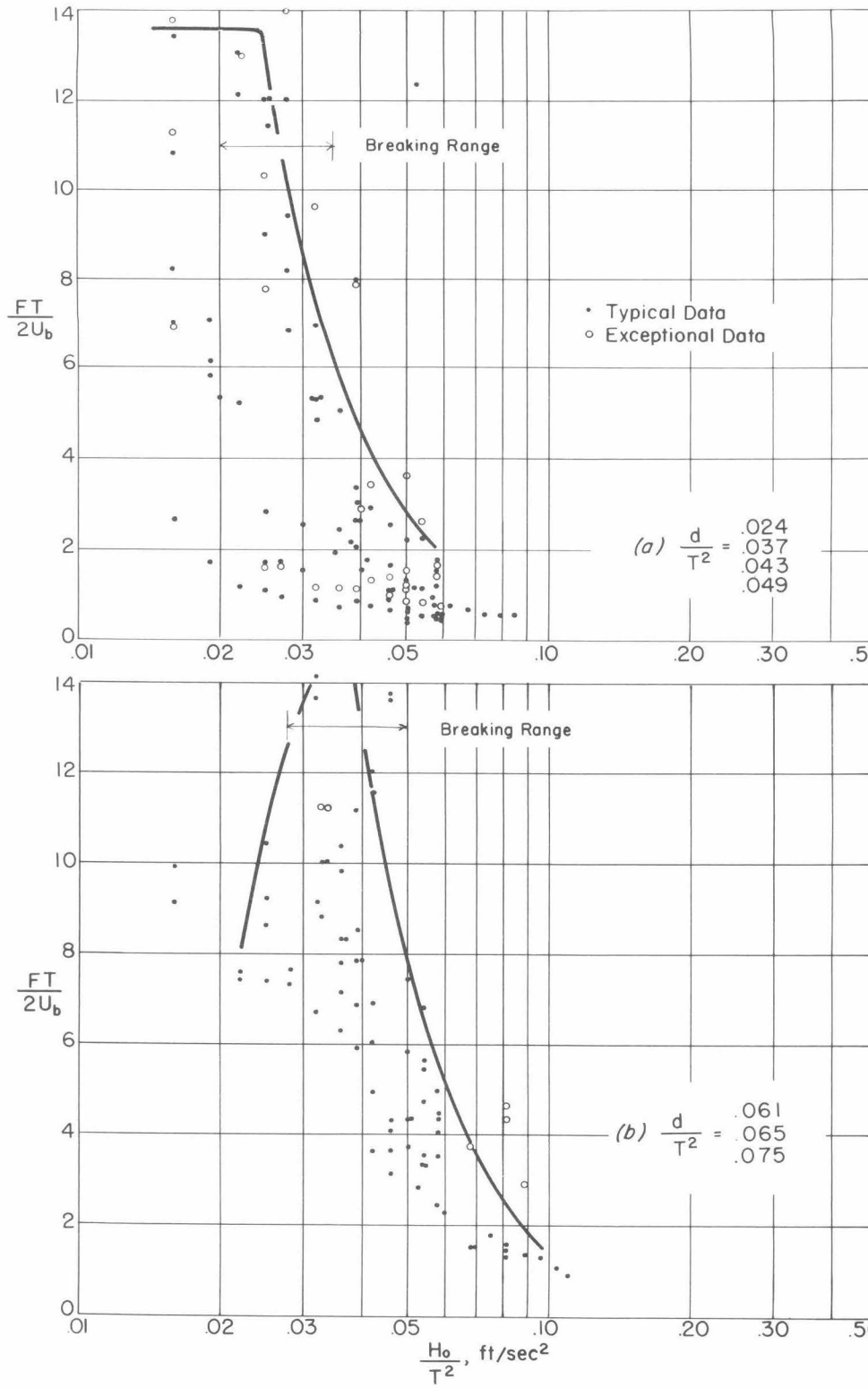

Fig. 9 - Dimensionless representation of force data, vertical barrier, 1:30 slope

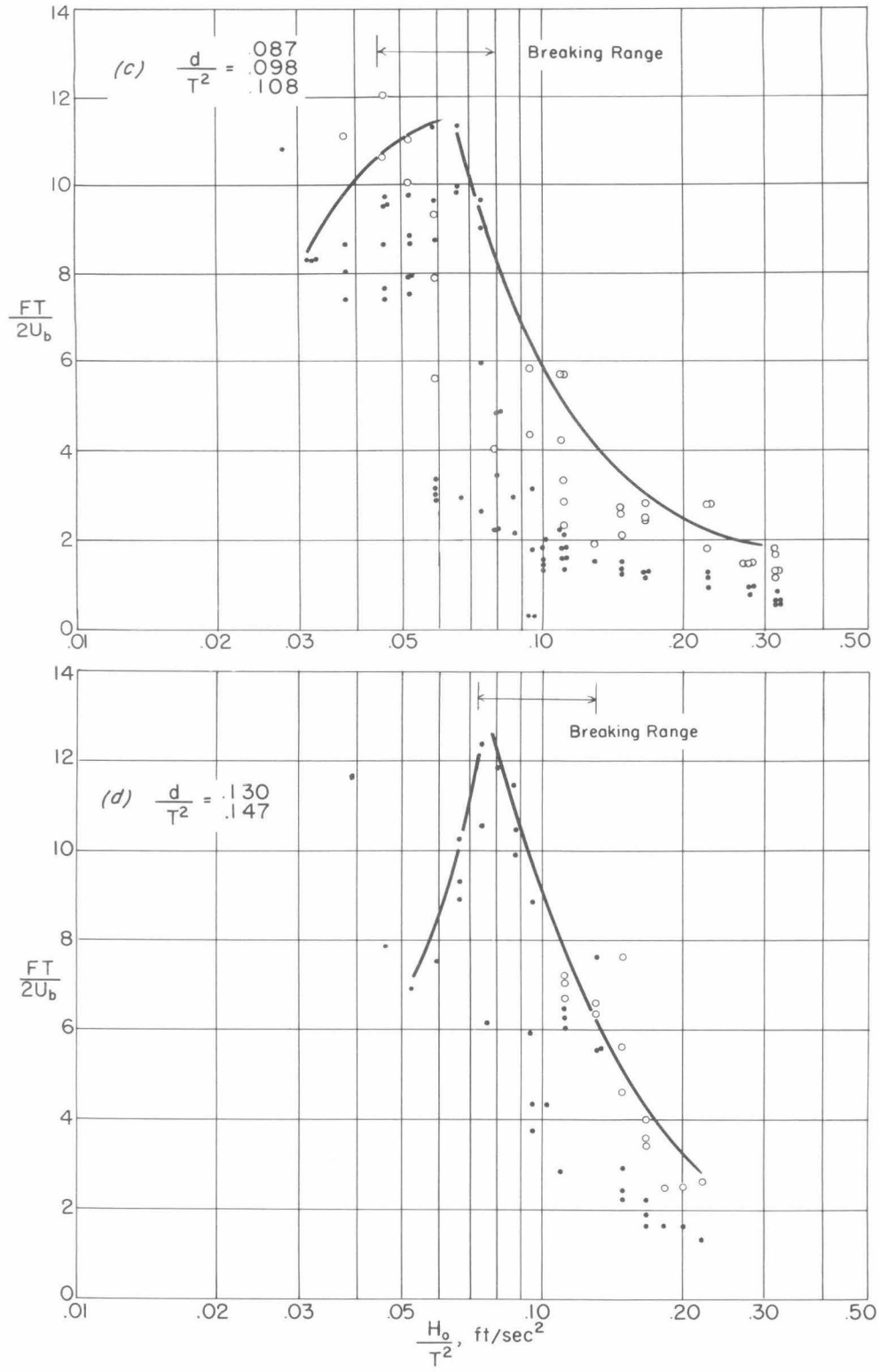

Fig. 9 (cont) - Dimensionless representation of force data, vertical barrier, 1:30 slope

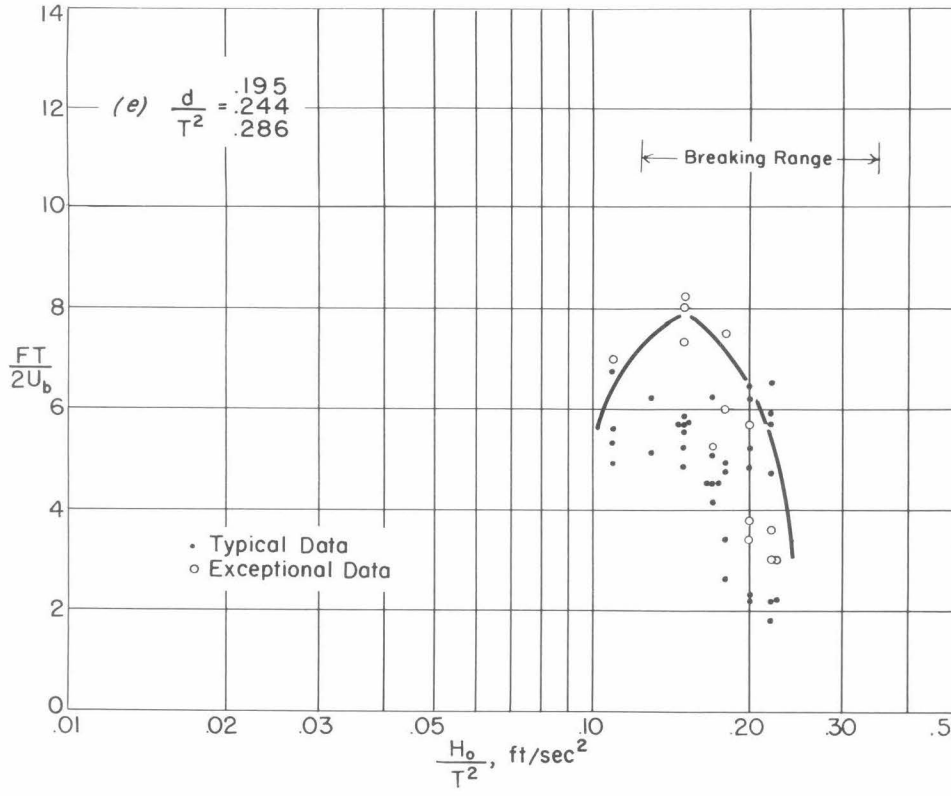

Fig. 9 (cont) - Dimensionless representation of force data, vertical barrier, 1:30 slope

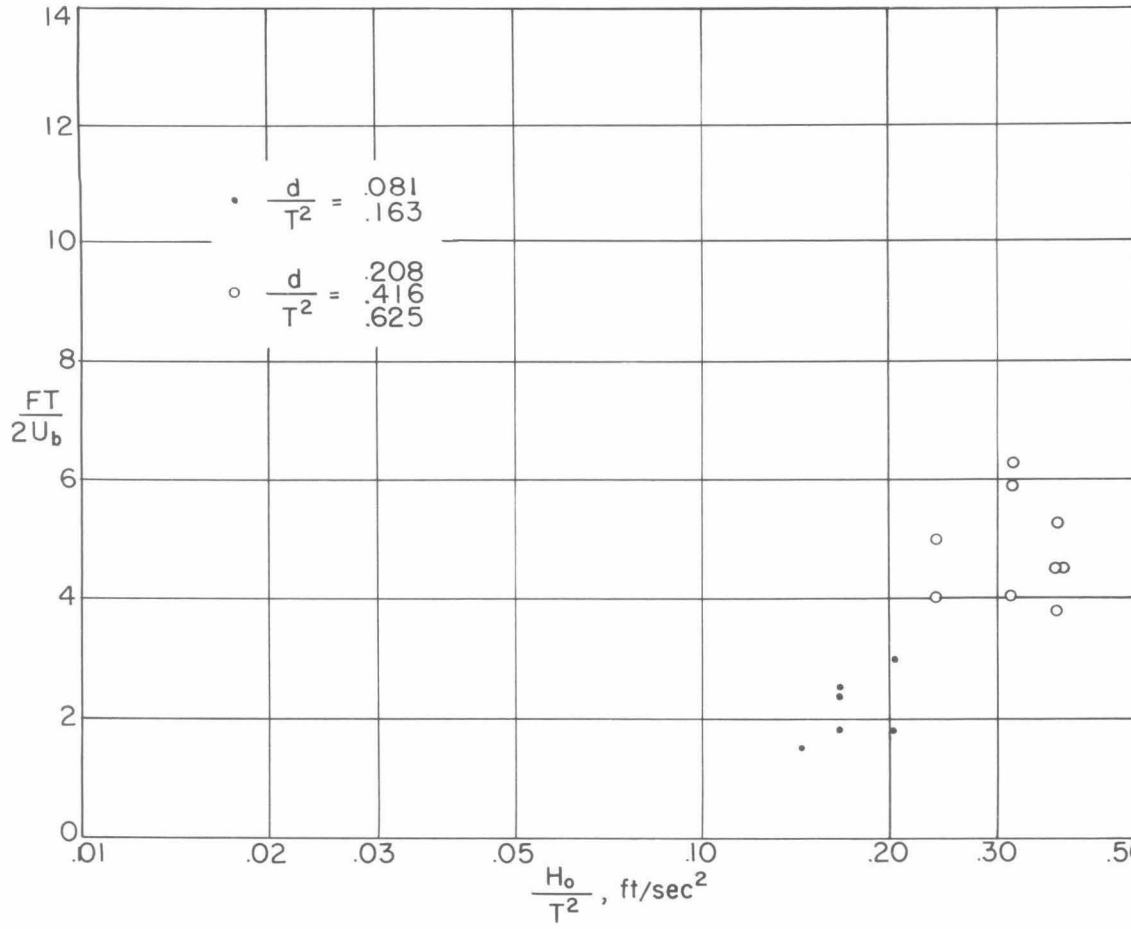

Fig. 10 - Dimensionless representation of force data, vertical barrier, 1:3 slope

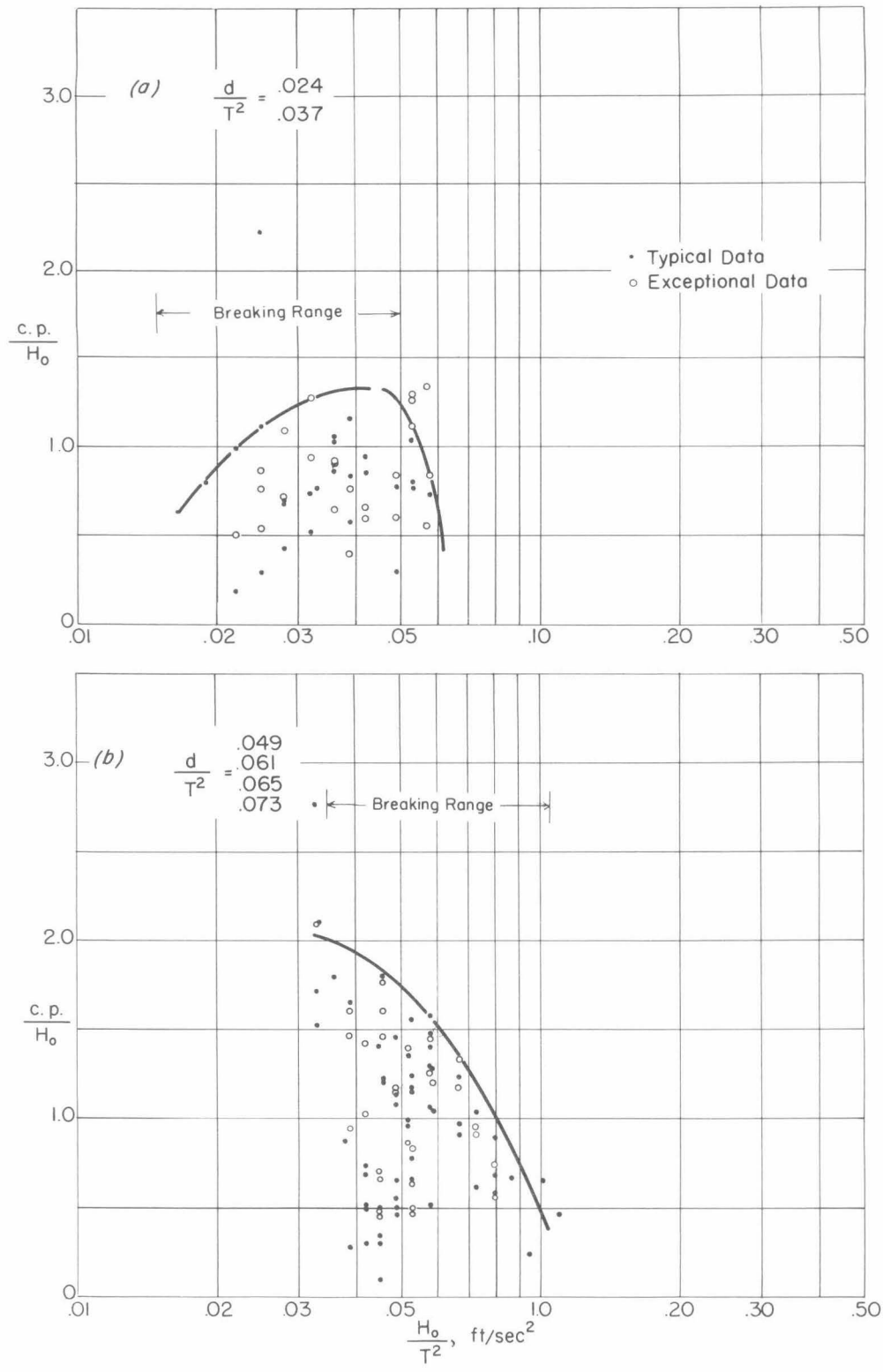

Fig. 11 - Dimensionless representation of moment data, vertical barrier, 1:10 slope

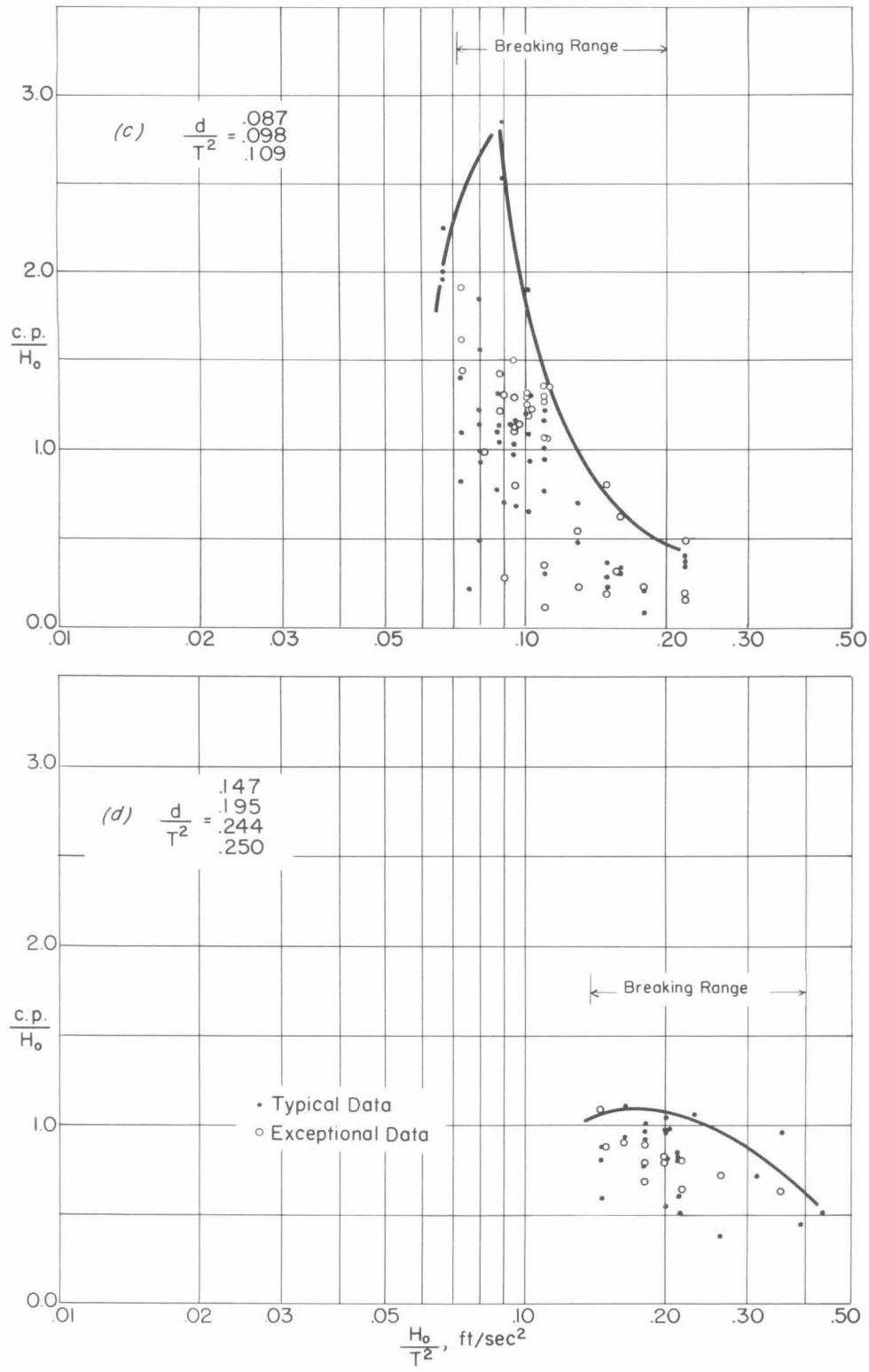

Fig. 11 (cont) - Dimensionless representation of moment data, vertical barrier, 1:10 slope

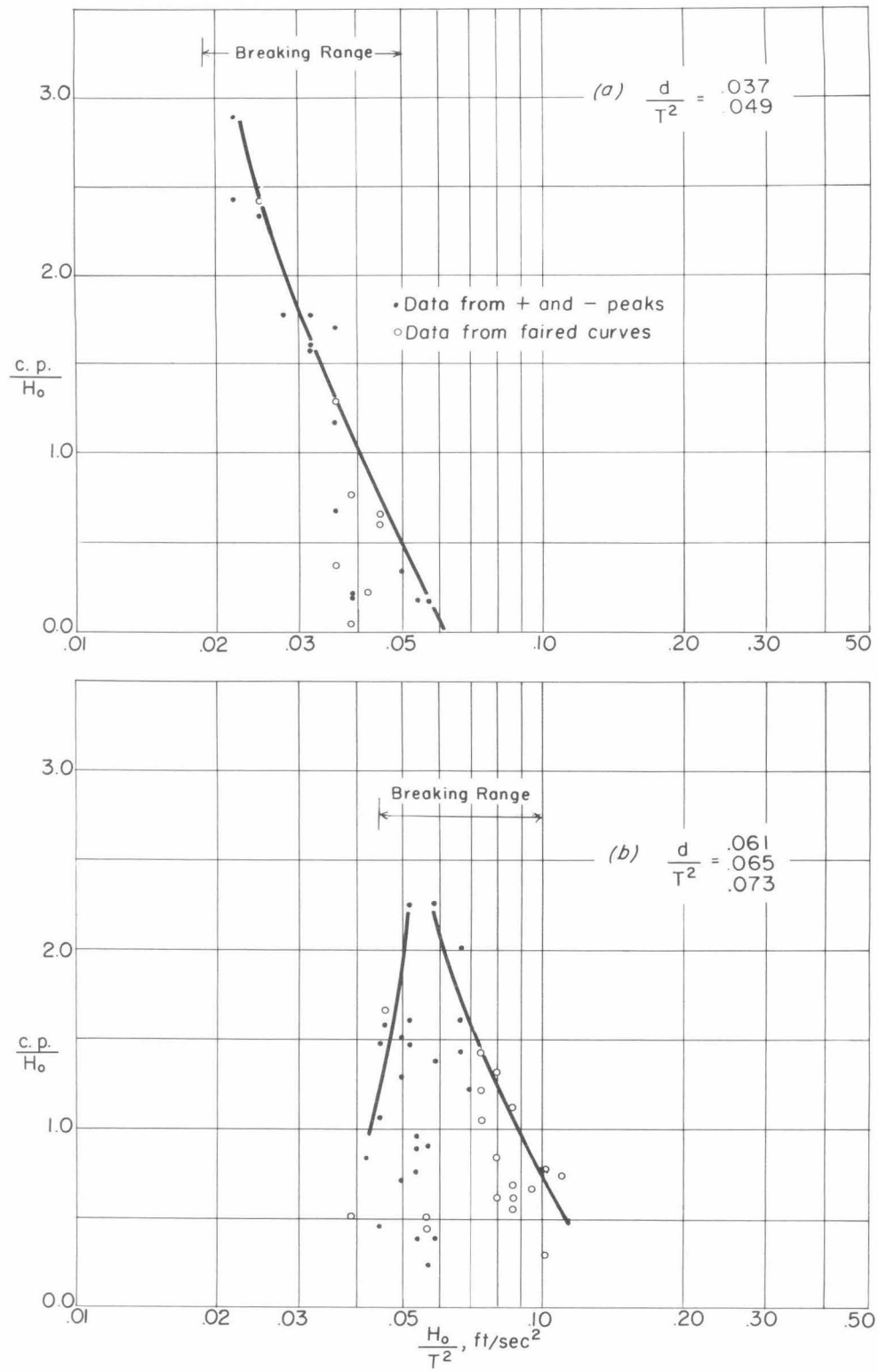

Fig. 12 - Dimensionless representation of moment data, 30° sloping barrier, 1:10 slope

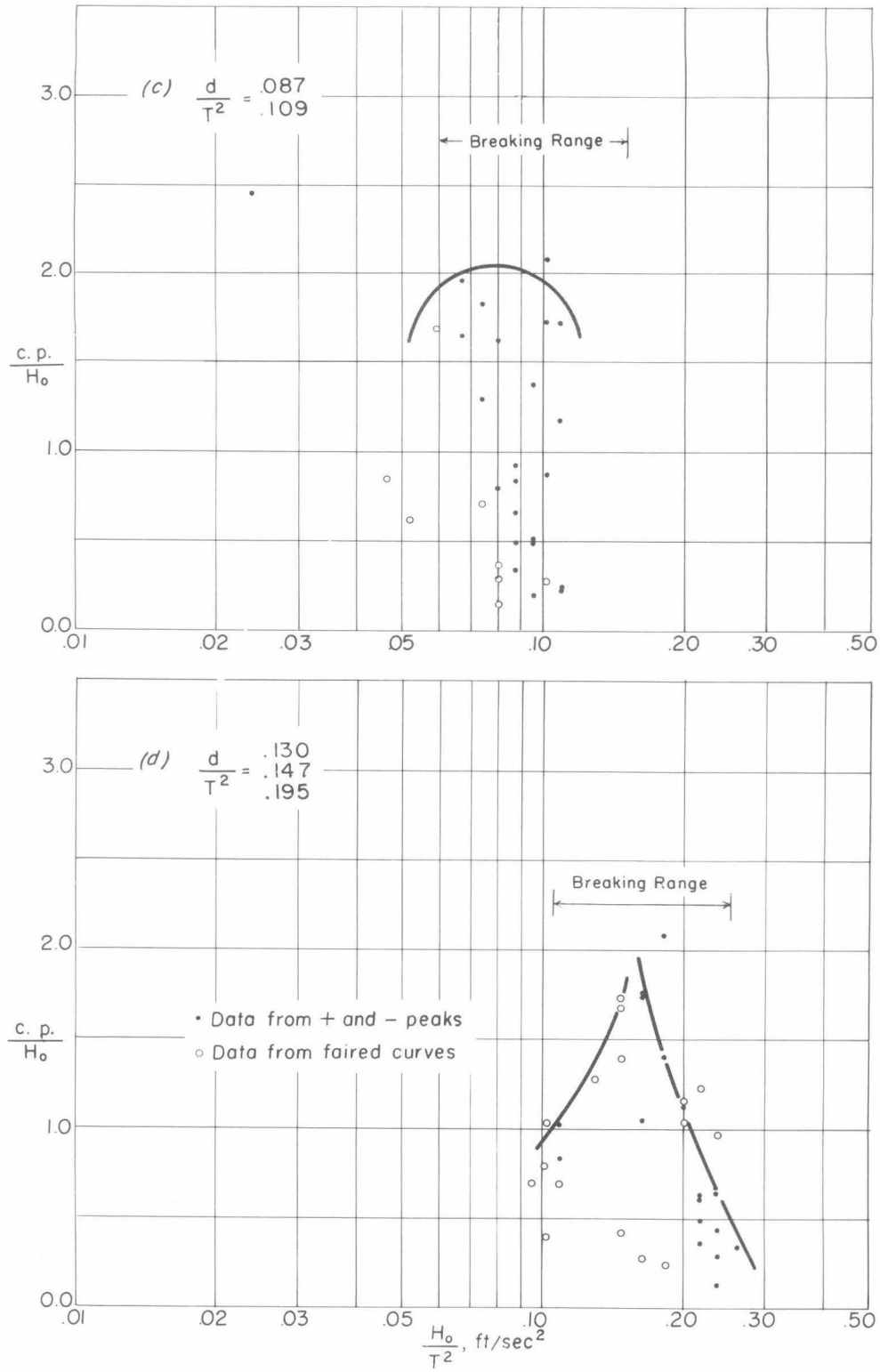

Fig. 12 (cont) - Dimensionless representation of moment data, 30^{o} sloping barrier, 1:10 slope

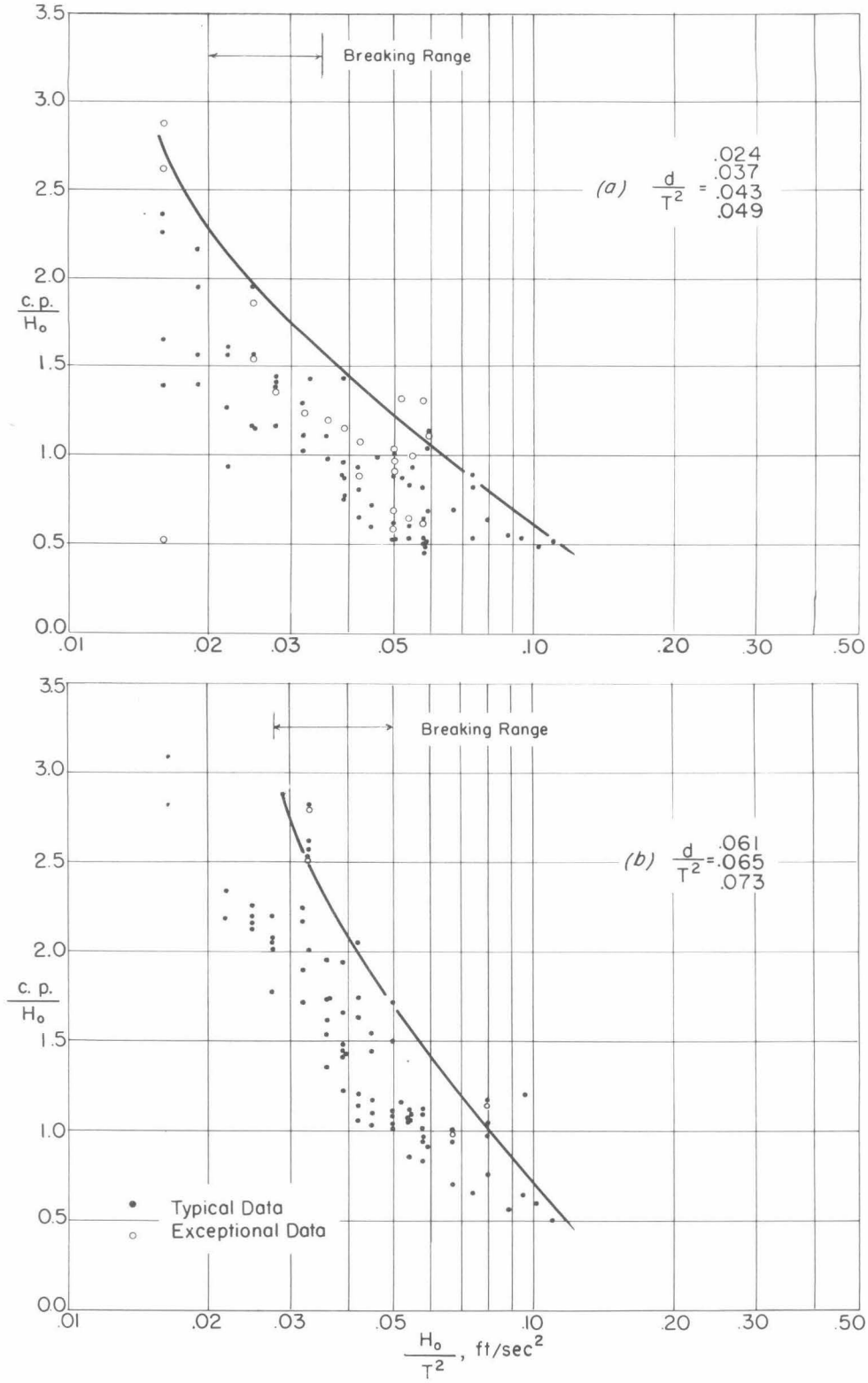

Fig. 13 - Dimensionless representation of moment data, vertical barrier, 1:30 slope

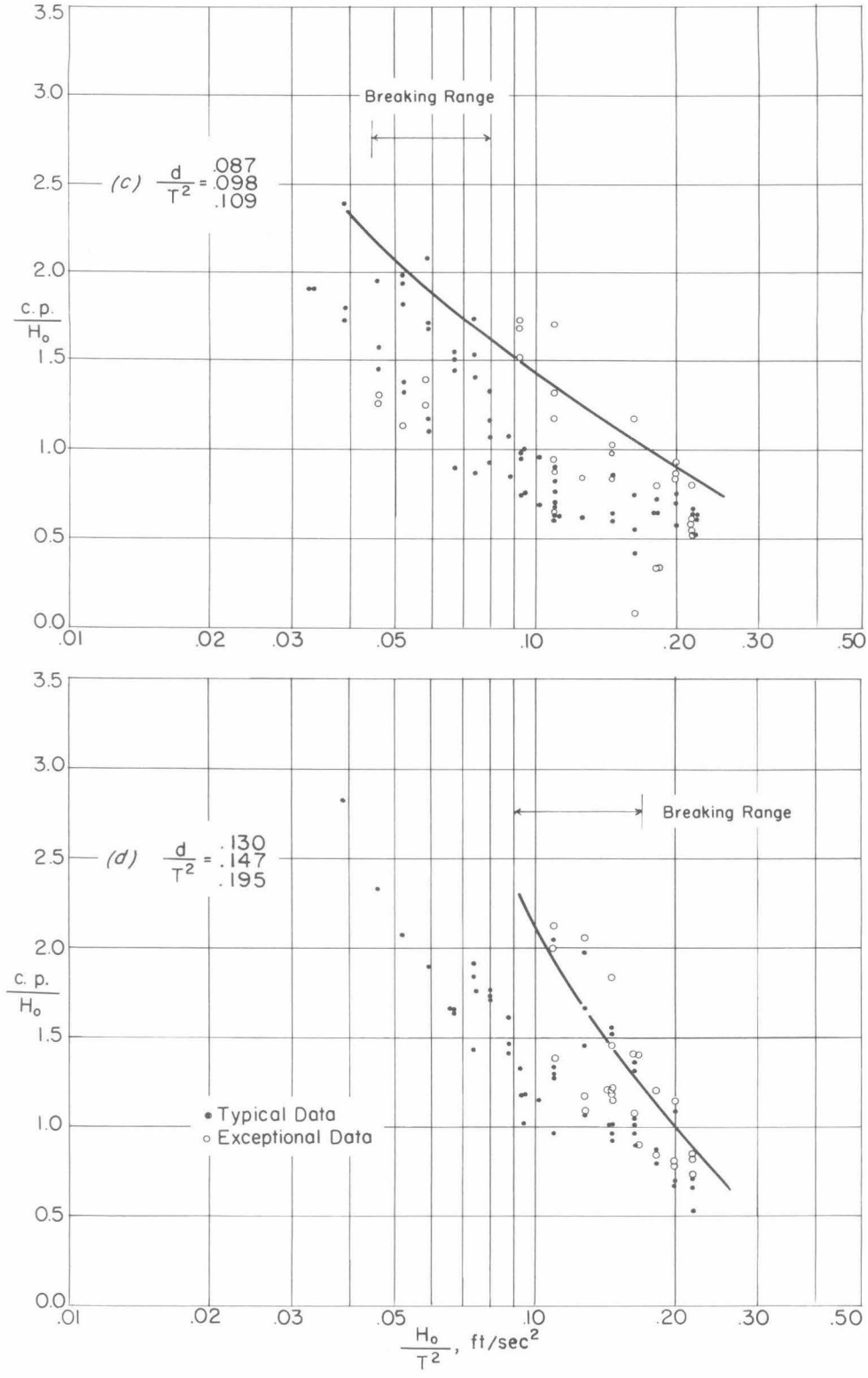

Fig. 13 (cont) - Dimensionless representation of moment data, vertical barrier, 1:30 slope

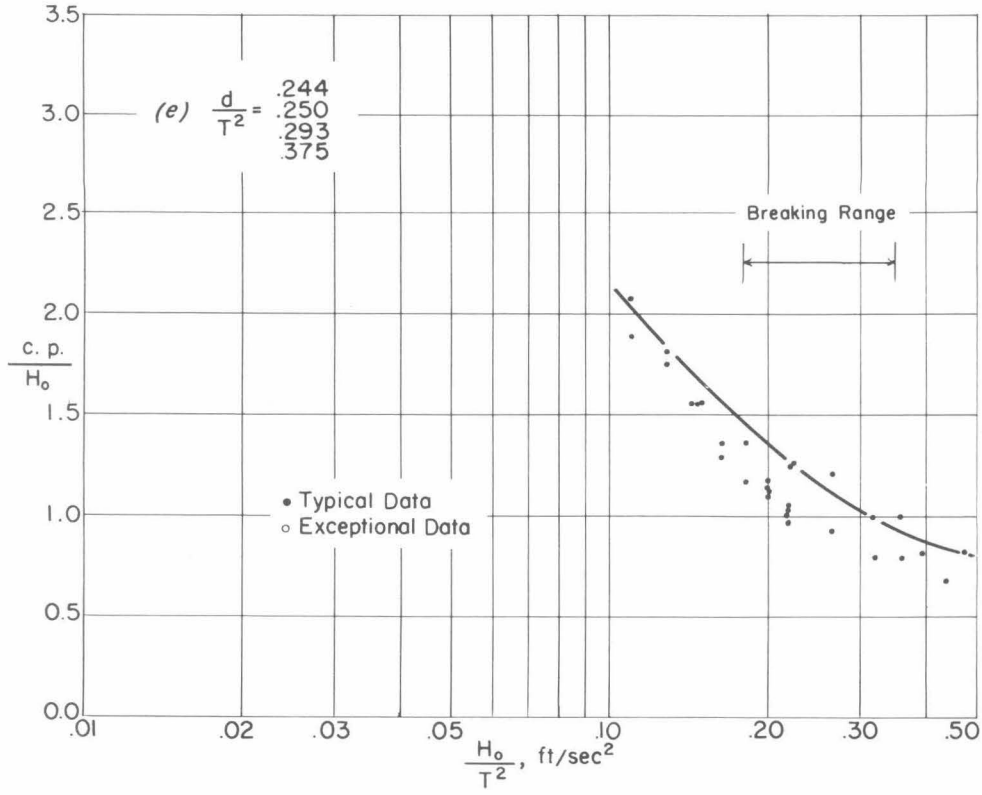

Fig. 13 (cont) - Dimensionless representation of moment data, vertical barrier, 1:30 slope

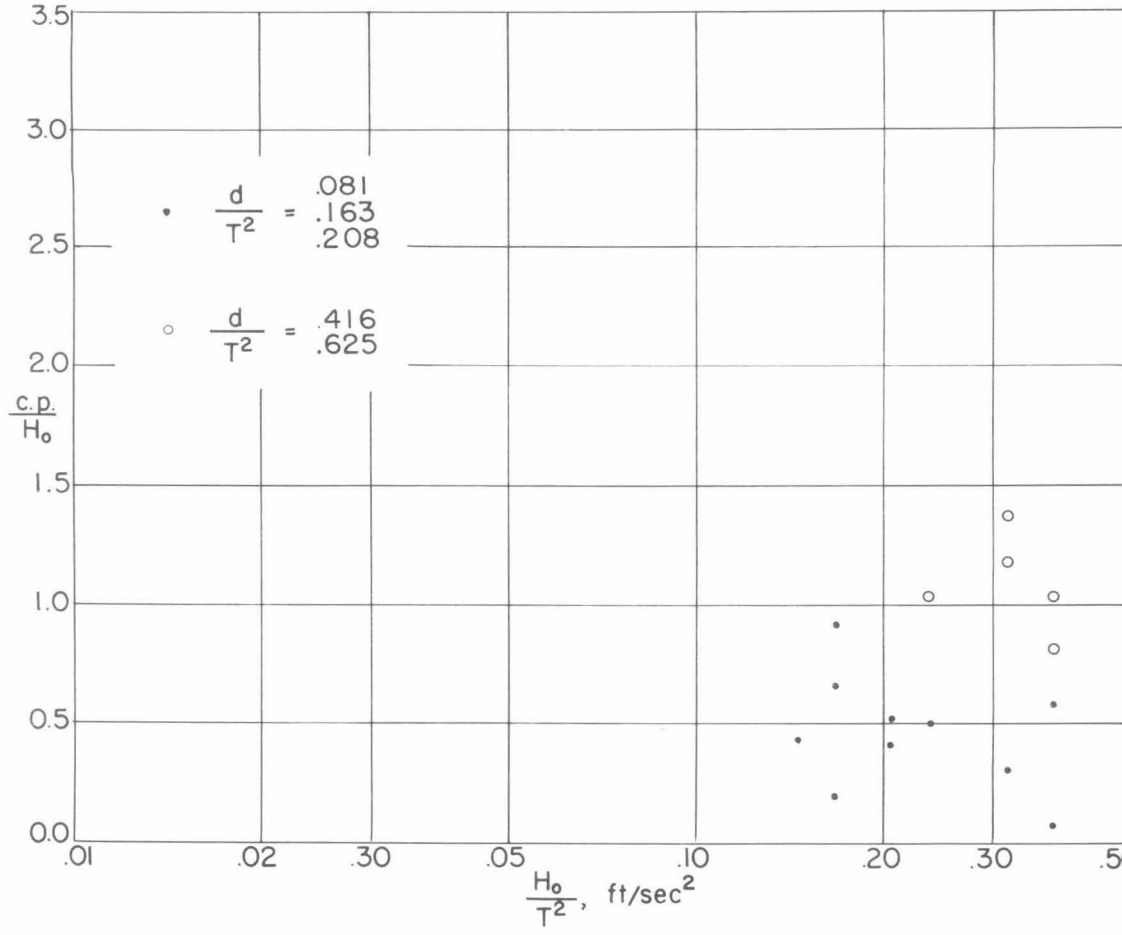

Fig. 14 - Dimensionless representation of moment data, vertical barrier, 1:3 slope

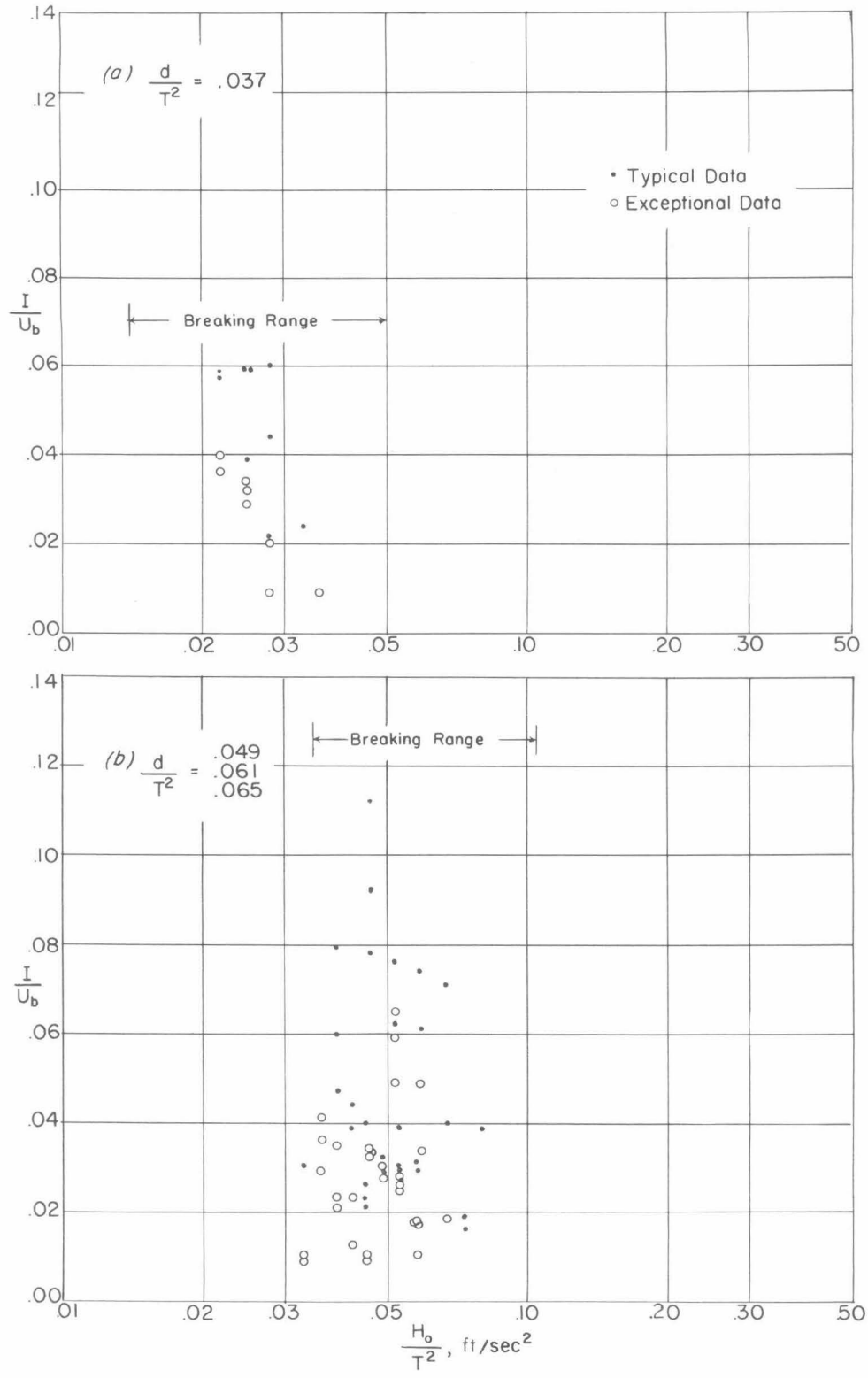

Fig. 15 - Shock impulse data, vertical barrier, 1:10 slope

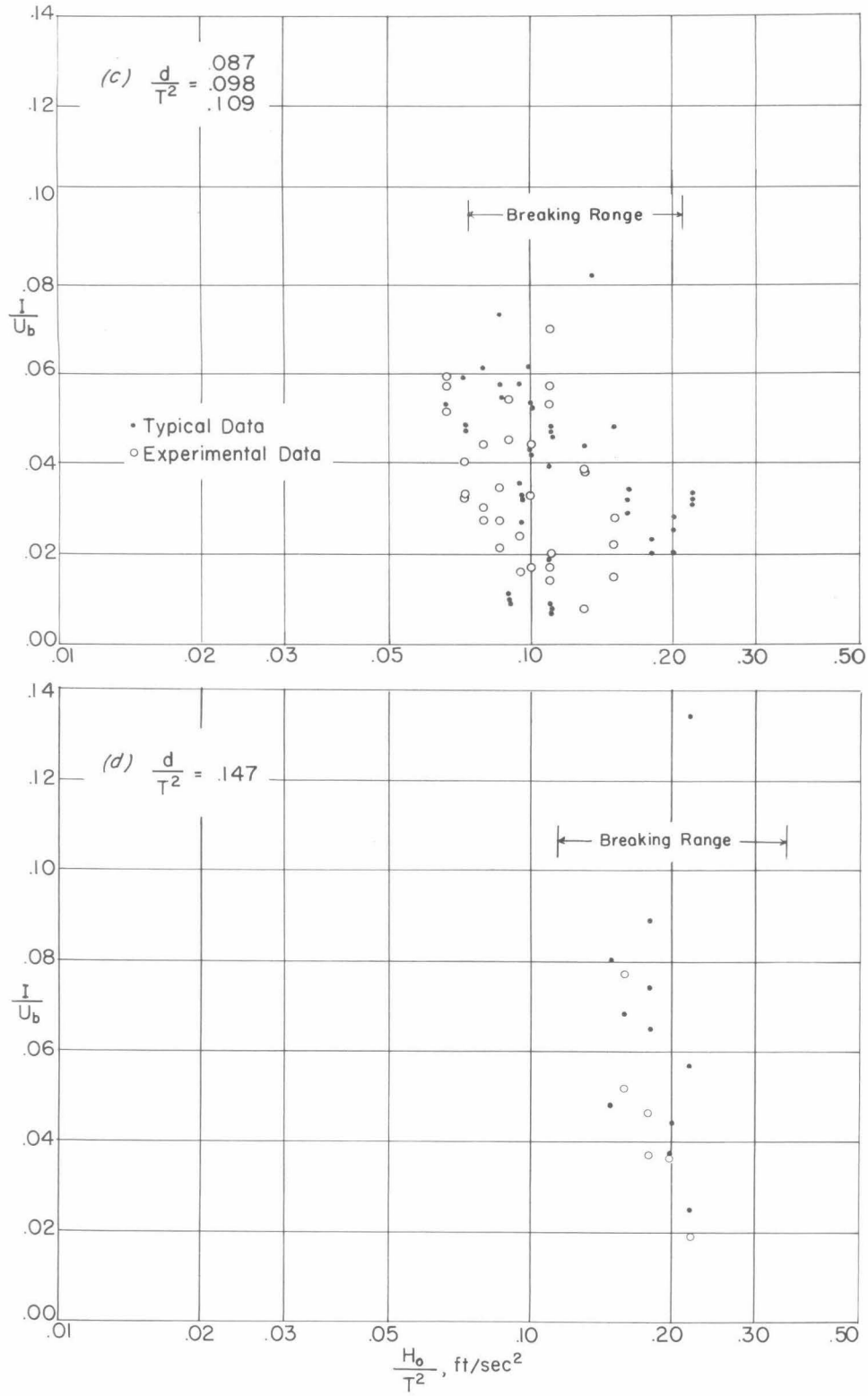

Fig. 15 (cont) - Shock impulse data, vertical barrier, 1:10 slope

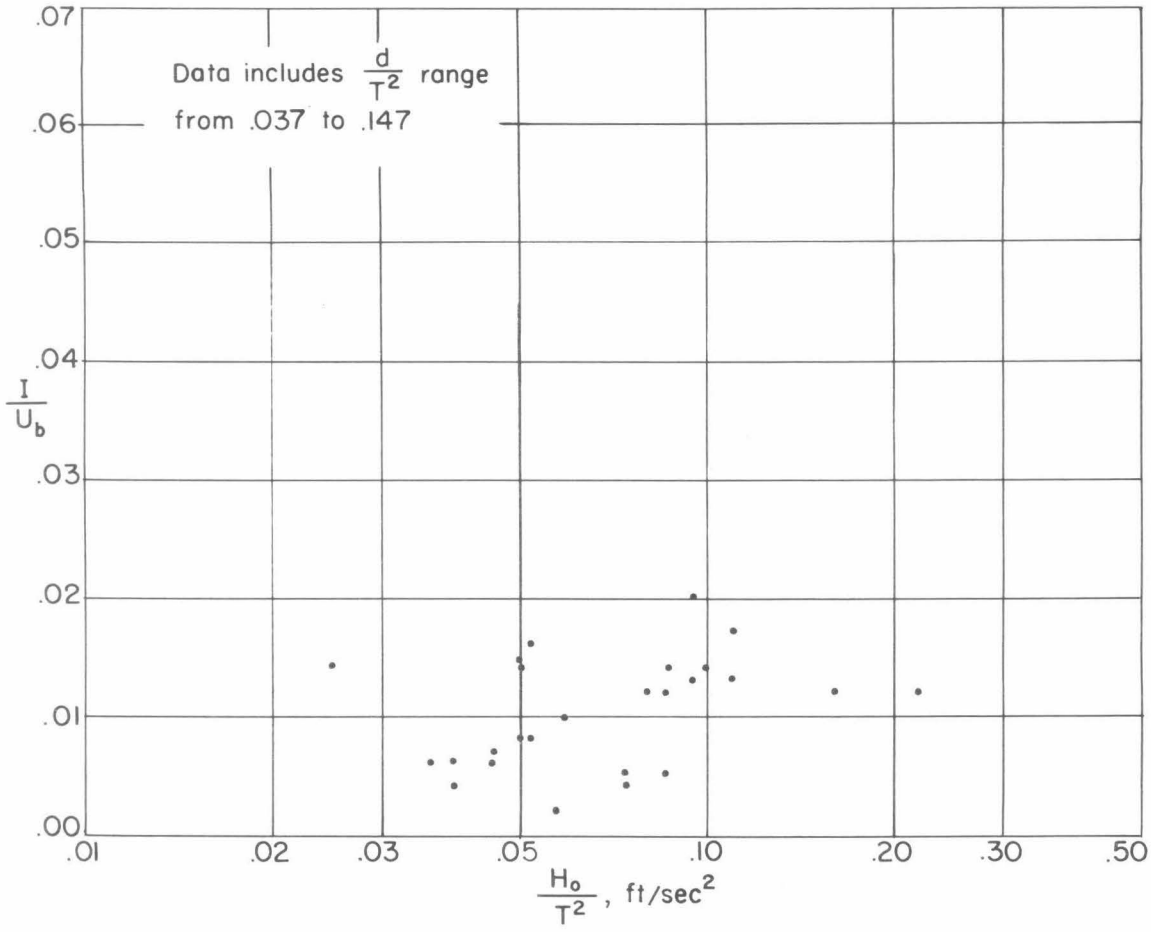

Fig. 16 - Shock impulse data, 30° sloping barrier, 1:10 slope

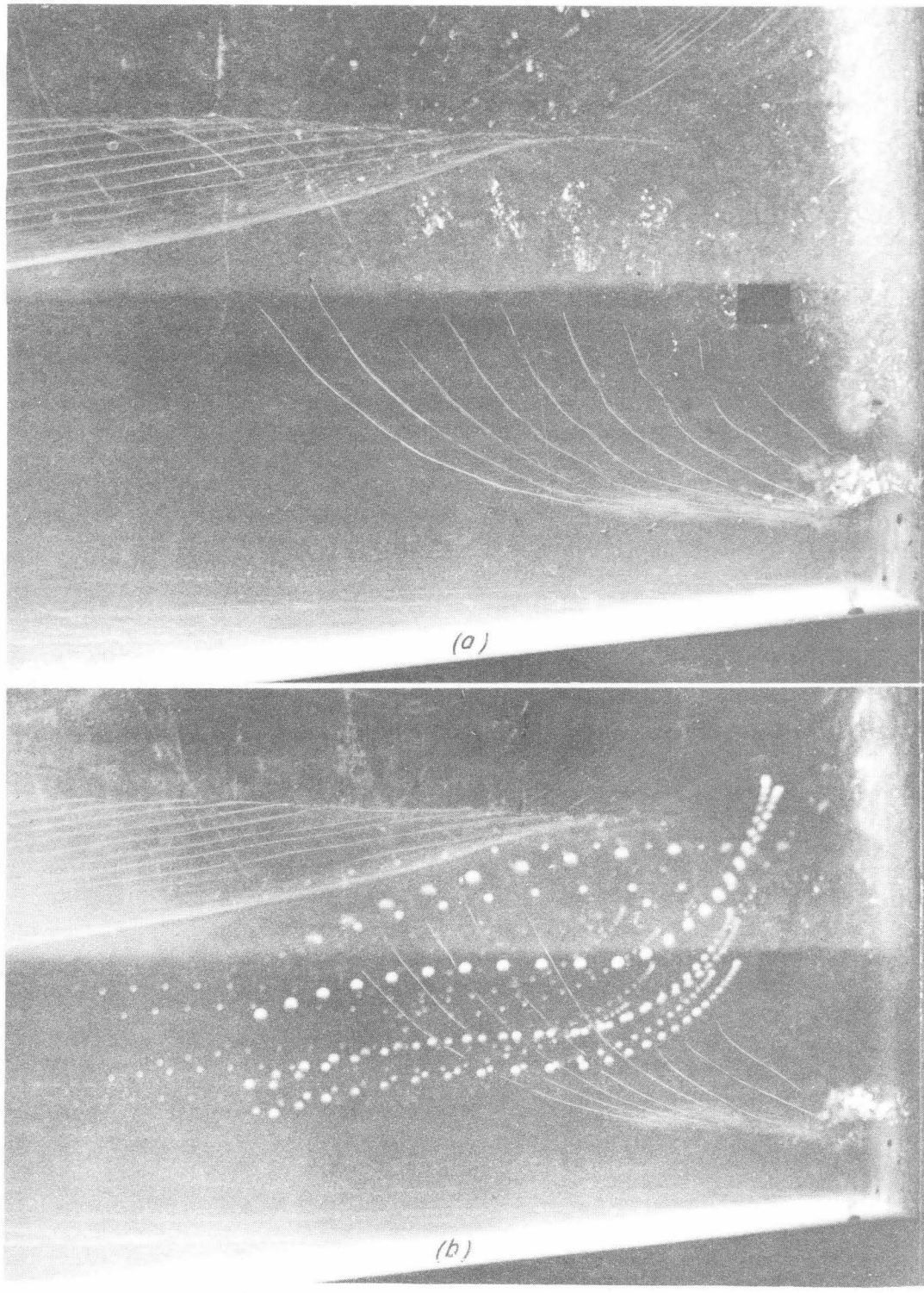

Fig. 17 - Breaking wave kinematics

(a) Surface profiles

(b) Particle motion